

AD-751 051

ASPECTS OF MECHANICAL BEHAVIOR OF ROCK
UNDER STATIC AND CYCLIC LOADING. PART A:
MECHANICAL BEHAVIOR OF ROCK UNDER STATIC
LOADING

Tarun Naik, et al

Wisconsin University

Prepared for:

Advanced Research Projects Agency

March 1972

DISTRIBUTED BY:

NTIS

National Technical Information Service
U. S. DEPARTMENT OF COMMERCE
5285 Port Royal Road, Springfield Va. 22151

**BEST
AVAILABLE COPY**

ENGINEERING EXPERIMENT STATION

AD 751051

ASPECTS OF MECHANICAL BEHAVIOR OF ROCK UNDER STATIC AND CYCLIC LOADING

Part A Mechanical Behavior of Rock under Static Loading

Annual Technical Progress Report
March 1972

Sponsored by Advanced Research Projects Agency
and monitored by U. S. Bureau of Mines
under Contract No. HO210004

ARPA Order No. 1579, Amendment 2
Program Code 1710



DDC
RECEIVED
NOV 13 1972
REGULATORY
B

Reproduced by
NATIONAL TECHNICAL
INFORMATION SERVICE
U S Department of Commerce
Springfield VA 22151

DISTRIBUTION STATEMENT A
Approved for public release
Distribution Unlimited


103

Mar 7, 66

Security Classification

DOCUMENT CONTROL DATA - R & D

(Security classification of title, body of abstract and indexing annotation must be entered when the overall report is classified)

1. ORIGINATING ACTIVITY (Corporate author)		2a. REPORT SECURITY CLASSIFICATION	
Engineering Experiment Station University of Wisconsin Madison, Wisconsin 53706		Unclassified	
3. REPORT TITLE		2b. GROUP	
Aspects of Mechanical Behavior of Rock under Static and Cyclic Loading. Part A - Mechanical Behavior of Rock under Static Loading.			
4. DESCRIPTIVE NOTES (Type of report and inclusive dates)			
Annual Technical Report			
5. AUTHOR(S) (First name, middle initial, last name)			
Tarun Naik, Robert G. Lundquist, Jesus Basas and Robert W. Heins			
6. REPORT DATE	7a. TOTAL NO. OF PAGES	7b. NO. OF REFS	
April 1972	90	10	
8a. CONTRACT OR GRANT NO.		8b. ORIGINATOR'S REPORT NUMBER(S)	
HO210004		144-B638	
9. PROJECT NO. ARPA Order No. 1579, Amendment No. 2 Program Code No. 1F10		8c. OTHER REPORT NO(S) (Any other numbers that may be assigned this report)	
10. DISTRIBUTION STATEMENT			
Distribution of this document is unlimited.			
11. SUPPLEMENTARY NOTES		12. SPONSORING MILITARY ACTIVITY	
Reproduced from  best available copy.		Advanced Research Projects Agency, Washington, DC 20301	
13. ABSTRACT			
Valders limestone was tested for indirect tensile strength using the well-known Brazilian test. The samples tested ranged in size from 3 in. in dia. by 2 in. long for the largest to 1 in. in dia. by 1/2 in. long for the smallest. Force vs. vertical displacement and force vs. horizontal strain at the center of the disc were plotted for each test specimen. No appreciable volume effect on the tensile strength of the specimens was apparent.			
A one-dimensional progressive failure model is proposed, consisting of linearly elastic springs in parallel which can deform independently of each other. The springs are assumed to be perfectly brittle and the values of stiffness and strength are assigned using the Monte Carlo technique. While this model is of no practical use, it does serve as a simple model to study the numerous variables involved.			
A two-dimensional progressive failure finite element model is presented. In this model the Brazilian test is modeled by a two-dimensional finite element structure. The following variables were analyzed: (1) ratio of allowable compressive strength to tensile strength, (2) number of loaded node points, (3) strength variance, and (4) stiffness variance. The two-dimensional model is capable of showing how failure develops in mixed stress fields, such as in Brazilian tests.			

DD FORM 1473
1 NOV 65I
-8-

Security Classification

14. KEY WORDS	LINK A		LINK B		LINK C	
	HOLE	WT	HOLE	WT	HOLE	WT
finite element analysis Brazilian test indirect tensile strength model of rock failure force-displacement curve bounded distributions of strength and stiffness finite element progressive failure model						

II

ASPECTS OF MECHANICAL BEHAVIOR OF ROCK UNDER
STATIC AND CYCLIC LOADING

PART A: MECHANICAL BEHAVIOR OF ROCK UNDER STATIC LOADING

ANNUAL TECHNICAL PROGRESS REPORT
MARCH 1972

by

R. W. Heins (Co-Principal Investigator
with B. C. Haimson)

Department of Metallurgical & Mineral Engineering
and the
Engineering Experiment Station
College of Engineering
The University of Wisconsin
Madison, Wisconsin 53706

Details of illustrations in
this document may be better
studied on microfiche

ARPA Order No. 1579, Amendment 2
Program Code No. 1F10, Contract No. H0210004
Contract Period: January 29, 1971 through February 28, 1972
Total Amount of Contract: \$47,985
Sponsored by ARPA and Monitored by U. S. Bureau of Mines

Disclaimer:

The views and conclusions contained in this document are those of the author and should not be interpreted as necessarily representing the official policies, either expressed or implied, of the Advanced Research Projects Agency or the U. S. Government.

III

PREFACE

This report covers the first year accomplishments in the research program entitled, "Mechanical Behavior of Rock Under Static Loading," R. W. Heins -Co-Principal Investigator. The program is Part A of the project entitled, "Aspects of Mechanical Behavior of Rock Under Static and Cyclic Loading" (Contract H0210004). Part B of the project is published in a separate volume.

ACKNOWLEDGEMENTS

The reported research was supported by ARPA, and monitored by Mr. Egon S. Podnieks of the Twin Cities Mining Research Center, U. S. Bureau of Mines. His cooperation and that of Dr. S. Peng are gratefully acknowledged.

The graduate research assistant who was responsible for the basic idea and who has done much of the work is Robert G. Lundquist. The remainder of the work is the responsibility of two postdoctoral fellows, Tarun Naik and Jesus Basas.

V

SUMMARY

ASPECTS OF MECHANICAL BEHAVIOR OF ROCK UNDER STATIC LOADING

PART A

Summary of Work to Date

Valders limestone was tested for indirect tensile strength using the well known Brazilian test. Various sizes of samples were tested. The largest sample was three inches in diameter by two inches long (3" x 2"), and the smallest was one inch in diameter by one-half inch long (1" x 1/2"). Results of these tests are summarized in Table 1. 4. 1. Force versus vertical displacement and force versus horizontal strain at the center of the disc were plotted for each test specimen. A closed-loop servocontrolled machine (MB machine) was used for the test. Application of load was controlled by lateral strain rate at the center of the disc. Complete stress-strain (force-displacement) curves were obtained.

A one-dimensional progressive failure model is given in Chapter 2. This model consists of linearly elastic springs in parallel. The springs deform independently of each other. They are assumed to be perfectly brittle, i. e., any additional load (force or displacement loading) beyond the peak will cause a sudden failure of the spring. The spring stiffness and strength (failure displacement) values are assigned to the elements by the Monte Carlo technique, using various types of probability distribution functions. Five types of distribution functions, Uniform, Left-skewed, Right-skewed, Uni-model and Bi-model, are used. The one-dimensional model computer program is given in Appendix A. The following variables were analyzed: (1) number of springs, (2) strength variance, (3) strength distribution, (4) stiffness variance, and (5) stiffness distribution.

A two-dimensional progressive failure finite element model is given in Chapter 3. In this model, the Brazilian test was modeled by a

VI

11

two-dimensional finite element structure. Elastic properties and strength values for each element of the finite element model are assigned by Monte Carlo technique using a uniform distribution function. A series of elastic analyses were performed on this structure. In each cycle, the element with worst combination of principal stress and strength is found. Ninety-nine percent of this element stiffness is then subtracted from the entire structure stiffness. The elastic analysis is performed on this new structure, and the cycles are repeated until catastrophic failure occurs. The following variables are analyzed: (1) ratio of allowable compressive strength to tensile strength, (2) number of loaded node points, (3) strength variance, and (4) stiffness variance.

Conclusions

The following conclusions may be extrapolated from the limited amount of work presented in this report.

(1) In order to obtain a complete force-displacement curve for brittle materials, such as Valders limestone, the loading rate must be controlled by horizontal displacement (or strain) rate in order to avoid catastrophic failure at or very near the peak load.

(2) The variation in the volume of the Brazilian test samples did not appear to have any significant effect upon the tensile strength of Valders limestone. The variation in average tensile strength was 3.7% around the mean value.

(3) The one-dimensional model does not have any direct use in practice, but it serves a very important use in this study. It serves as a simple model to study numerous variables involved.

(4) The strength variance and the shape of the strength distribution has a marked effect upon the force-displacement curves. On the other hand, the stiffness variance and the shape of the stiffness distribution does not have a very significant effect upon the force-displacement curves.

VII

(5) The use of bounded distribution functions allows the effect of variables to be examined with physical interpretations to be placed on these bounds.

(6) While the two-dimensional model gives good qualitative results, it should not be considered a quantitative tool for solving rock mechanics problems until further modifications and improvisations are made.

(7) The two-dimensional model is capable of showing how failure develops in mixed stress fields such as Brazilian tests.

Future Work

The general direction of the future program will be as follows:

(1) Additional Brazilian tests on Valders limestone will be performed.

(2) Two other rock types, Dacite and St. Cloud Gray granodiorite, will be also used for Brazilian tests.

(3) Additional work on the two-dimensional model will be performed. Work is underway on a two-dimensional model using isoparametric finite elements, automatic mesh generation, and other refinements. Anisotropy of elements will also be included.

(4) Other types of two-dimensional models are also planned. The greatest emphasis will be placed upon new failure criterion. Literature search is underway.

(5) After a new, improvised, two-dimensional model is developed, work on a three-dimensional model will be started.

TABLE OF CONTENTS

PREFACE	1
ACKNOWLEDGEMENTS	ii
SUMMARY	iii
TABLE OF CONTENTS	vi
LIST OF FIGURES	vii
LIST OF TABLES	viii
CHAPTER 1 - BRAZILIAN TEST ON VALDERS LIMESTONE	1
1. 1 Introduction	1
1. 2 Brazilian Test	1
1. 3 Sample Size	3
1. 4 Test Procedure and Results	3
1. 5 Discussion of Results	19
1. 6 Conclusions	20
1. 7 Future Program	21
Bibliography	21
CHAPTER 2 - ONE-DIMENSIONAL MODEL	22
2. 1 Introduction	22
2. 2 Distribution Functions	22
2. 3 Progressive Failure Model	23
2. 4 Discussion of Results	24
2. 5 Observations	41
Bibliography	42
CHAPTER 3 - TWO-DIMENSIONAL MODEL	43
3. 1 Introduction	43
3. 2 The Model	44
3. 3 Test of the Model	45
3. 4 Test Results	48
3. 5 Conclusions	56
Bibliography	62
APPENDIX A - ONE-DIMENSIONAL PROGRAM	63
APPENDIX B - TWO-DIMENSIONAL PROGRAM	72

IX

VI

LIST OF FIGURES

FIGURE 1. 2. 1	Brazilian Test	2
FIGURE 1. 4. 1	The MB Universal Testing Machine	4
FIGURE 1. 4. 2	Vertical Displacement Measurement Device	6
FIGURE 1. 4. 3	Horizontal Displacement Measurement Device	7
FIGURE 1. 4. 4	Brazilian Test Sample	8
FIGURE 1. 4. 5	Brazilian Test	9
FIGURE 1. 4. 6	Vertical Force Versus Vertical Displacement Specimen 34T	13
FIGURE 1. 4. 7	Vertical Force Versus Horizontal Strain at the Center of Disc, Specimen 34T	14
FIGURE 1. 4. 8	Sample 29T After Failure	15
FIGURE 1. 4. 9	Sample 18T After Failure	16
FIGURE 1. 4. 10	Sample 7M After Failure	17
FIGURE 1. 4. 11	Sample 31T After Failure	18
FIGURE 2. 4. 1	Effect of N, Number of Spring Elements, N = 10.	26
FIGURE 2. 4. 2	Effect of N, N = 100	27
FIGURE 2. 4. 3	Effect of N, N = 500	28
FIGURE 2. 4. 4	Effect of N, N = 1000	29
FIGURE 2. 4. 5	Effect of N Compared, N = 10, 100, 500, 1000	30
FIGURE 2. 4. 6	Effect of B_s , Upper Limit of Strength Distribution	31
FIGURE 2. 4. 7	Effect of A_s , Lower Limit of Strength Distribution	33
FIGURE 2. 4. 8	Strength Distribution Uniform	34
FIGURE 2. 4. 9	Strength Distribution Unimodal	35
FIGURE 2. 4. 10	Strength Distribution Left-Skewed	36
FIGURE 2. 4. 11	Strength Distribution Right-Skewed	37
FIGURE 2. 4. 12	Strength Distribution Bimodal	38
FIGURE 2. 4. 13	Effect of V_k , Stiffness Variance	39
FIGURE 2. 4. 14	Effect of Varying Stiffness Distribution	40
FIGURE 3. 3. 1	Brazilian Test Finite Element Mesh	47

FIGURE 3. 4. 1	Progression of Failure in Test A-2	49
FIGURE 3. 4. 2	Vertical Force-Displacement for Test A-2	50
FIGURE 3. 4. 3	Progression of Failure in Test A-3	52
FIGURE 3. 4. 4	Vertical Force-Displacement for Test A-3	53
FIGURE 3. 4. 5	Progression of Failure in Test A-4	54
FIGURE 3. 4. 6	Vertical Force-Displacement for Test A-4	55
FIGURE 3. 4. 7	Progression of Failure in Test A-5	57
FIGURE 3. 4. 8	Vertical Force-Displacement for Test A-5	58
FIGURE 3. 4. 9	Progression of Failure in Test A-6	59
FIGURE 3. 4. 10	Vertical Force-Displacement for Test A-6	60
FIGURE 3. 4. 11	Vertical Force Vs. Horizontal Strain for Test A-3	61

LIST OF TABLES

TABLE 1. 4. 1	Results of Brazilian Tests on Valders Limestone Under Horizontal Strain Rate Controlled Loading	11
TABLE 2. 2. 1	Statistics for the Five Distributions	23
TABLE 3. 4. 1	Brazilian Test Conditions	51

XII

PART A

**ASPECTS OF MECHANICAL BEHAVIOR OF ROCK
UNDER STATIC AND CYCLIC LOADING**

A FINITE ELEMENT MODEL OF ROCK FAILURE FROM THE BRAZILIAN TEST

**Tarun Naik
Robert G. Lundquist
Jesus Basas
Robert W. Heins**

March, 1972

**Department of Metallurgical & Mineral Engineering
The University of Wisconsin
Madison, Wisconsin 53706**

XII

CHAPTER 1

BRAZILIAN TEST ON VALDERS LIMESTONE

1. 1 Introduction

Valders limestone was tested for indirect tensile strength using the well-known Brazilian test. Various sizes of samples were tested. The largest sample was three inches in diameter by two inches long (3" x 2"), and the smallest was one inch in diameter by one-half inch long (1" x 1/2"). Force versus vertical displacement and force versus horizontal strain at the center of the disc were plotted for each test specimen. A closed-loop servocontrolled machine (MB machine) was used for the test. Application of the load was controlled by lateral strain rate at the center of the disc.

The primary objective of the laboratory testing program was to obtain complete stress-strain (or force-displacement) curves for qualitative comparison with the mathematical models proposed in Chapters 2 and 3. The objective behind using various sizes of samples was to study the effect of the sample volume on the tensile strength as determined by the Brazilian test. It was also intended that the mathematical model would give similar qualitative information regarding the effect of the sample volume.

1. 2 Brazilian Test

The Brazilian test for measuring the tensile strength of brittle materials, like concrete, rocks, etc., is not only widely used in this country but in Europe and many other parts of the world also. It is probably the simplest test in terms of preparing the samples, carrying out the testing, and analyzing the results. A circular disc is cut from the material to be tested and is loaded by a theoretically concentrated line load, Figure 1. 2. 1. The stress

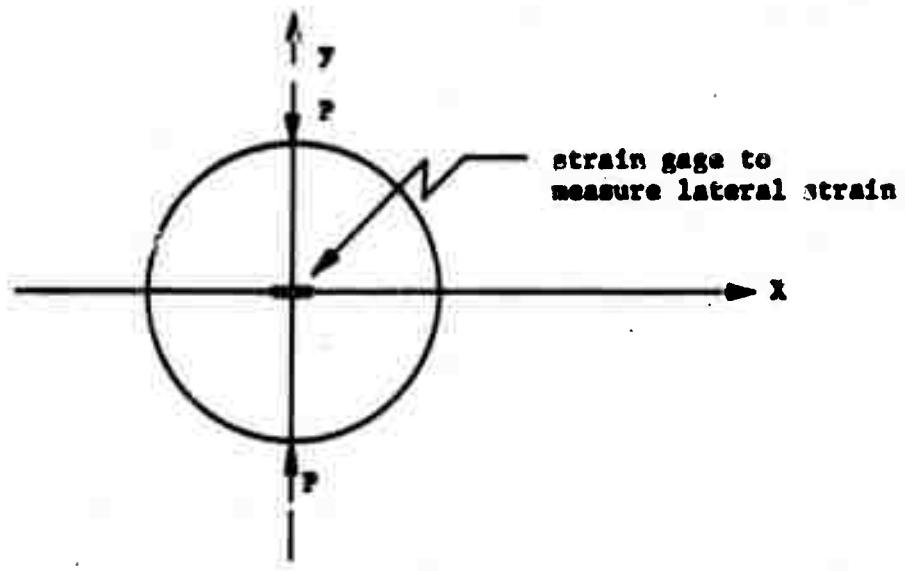


FIGURE 1. 2. 1 Brazilian Test

along the load axis in x direction is constant up to about $\pm 0.8 R$ from the center, and is given by Timoshenko and Goodier(1)* to be

$$S_t = \frac{P/t}{\pi R} = \frac{2P}{\pi Dt} \tag{1. 2. 1}$$

where

- S_t = tensile stress perpendicular to the load axis
- P = concentrated line load
- R = radius of the disc
- t = thickness of the disc, and
- D = diameter of the disc.

The dimensions of the specimen can be measured before the testing and the load P needed to fail the sample is recorded from the loading machine. Then, Equation 1. 2. 1 gives the tensile strength of the specimen.

The tensile strength of the specimen is obtained by Equation 1. 2. 1 if the failure is caused by excess tension along the load axis. However, many times the failure is initiated by a "crushing and wedging mechanism" at the point of application of the load P, Figure 1. 2. 1. Coates (2) gives an empirical relationship in order to take this mechanism into account. Fairhurst (3)

*Number in parenthesis indicates reference number in the bibliography at the end of this chapter.

has suggested that this "crushing and wedging" action can be avoided by applying the load over an arc of about 7° .

In the present laboratory investigation considering the samples run to date, the crushing was confined to a very small portion of the loading surface, thus Equation 1. 2. 1 was used to calculate the tensile strength.

1. 3 Sample Size

The sample sizes were decided based upon the following criteria:

1. The volume of the sample should be doubled each time, for the same diameter sample.
2. The failure load of the sample should not exceed the capacity of the machine (25 kips).
3. The diameter of the sample should be such that it fits into the vertical displacement measurement device, Figure 1. 4. 2, conveniently and easily.

The third criterion limited the samples to be three inches in diameter or less. The second criterion limited the largest sample size to be three inches in diameter by two inches in thickness (3" x 2"). Therefore, beginning with a sample 3" x 2", the following sample sizes were selected to meet the first criterion.

1. 3" diameter x 2", 1" and 1/2" thick,
2. 2" diameter x 2", 1" and 1/2" thick, and
3. 1" diameter x 2", 1" and 1/2" thick.

1. 4 Test Procedure and Results

A closed-loop servocontrolled machine (MB machine), Figure 1. 4. 1, was used for the Brazilian test of Valdars limestone. Application of load was controlled by the horizontal strain rate at the center of the sample disc. Applied force versus horizontal strain at the center output was directly recorded by the MB machine recorder, and a special additional plotter was used

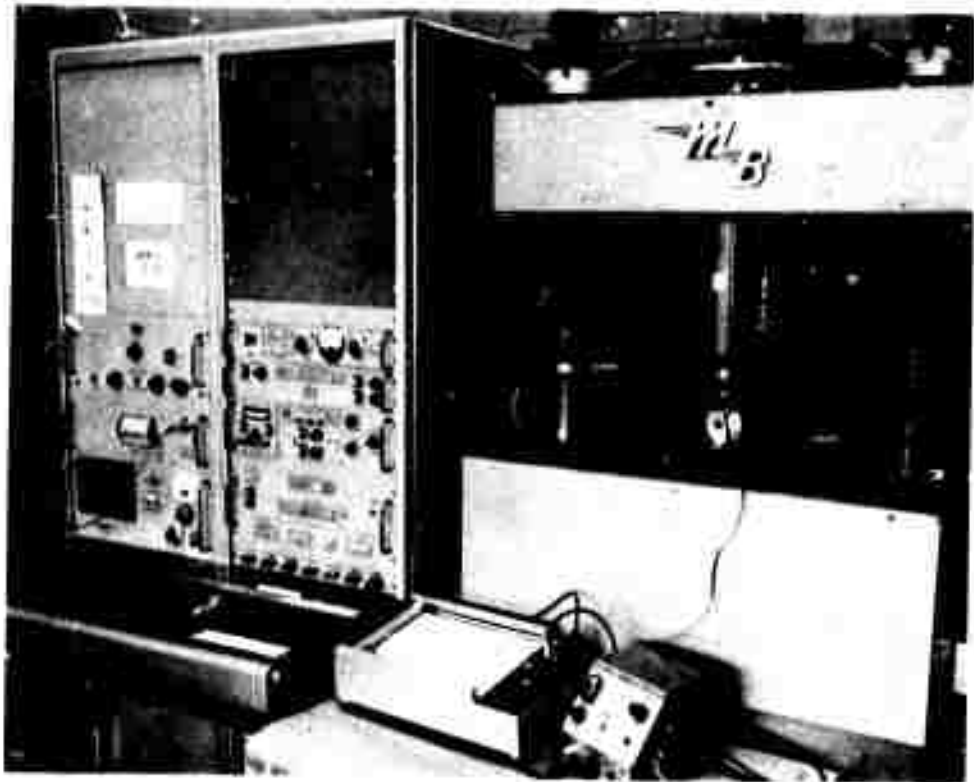


Figure 1.4.1 The MB Universal Testing Machine

(foreground, Figure 1. 4. 1) to plot force versus vertical displacement.

A special platen was constructed to measure the vertical displacement, Figure 1. 4. 2. The top and bottom plates were very carefully machined to make them perfectly horizontal such that no eccentricity will be introduced in the application of the vertical load. An adapter, to fit the platen at top into the load, was also very precisely made in order to have perfect, full contact with the load cell. One strain gage was mounted on top of each of the two cantilevers extending from the top platen. First, the cantilevers are pulled down by tightening the nuts on top of the two poles. As the bottom platen moves up, the cantilever will be displaced upward and will record a certain value of strain. The platen set was calibrated to convert strain on the cantilever to vertical movement of the platen.

To measure horizontal displacement on the axis perpendicular to the applied load, another displacement measuring mechanism was devised, Figure 1. 4. 3. A considerable amount of effort was spent on this device to perfect it in an attempt to make it give satisfactory results; however, satisfactory results were not obtainable and the device was discarded.

Because of sudden failure and permanent deformation of the device, it was decided to use strain gages directly mounted at the center of the rock, Figure 1. 4. 4. Two SR-4 strain gages were mounted on the sample, one each on the two faces of the disc, Figure 1. 4. 4. This alternative is expensive because two strain gages are expended for each sample tested, and is time consuming because considerable time is spent in mounting the strain gages. However, the strain gage method gives an accurate strain value at the center of the disc. The average of the two strain gage readings was used in the force versus horizontal strain plots.

After the samples were cored and cut to proper sizes, they were dried in an oven for 48 hours. Two strain gages, one on each side, were then mounted in the standard manner. The sample was positioned in the loading frame and carefully centered, Figure 1. 4. 5.

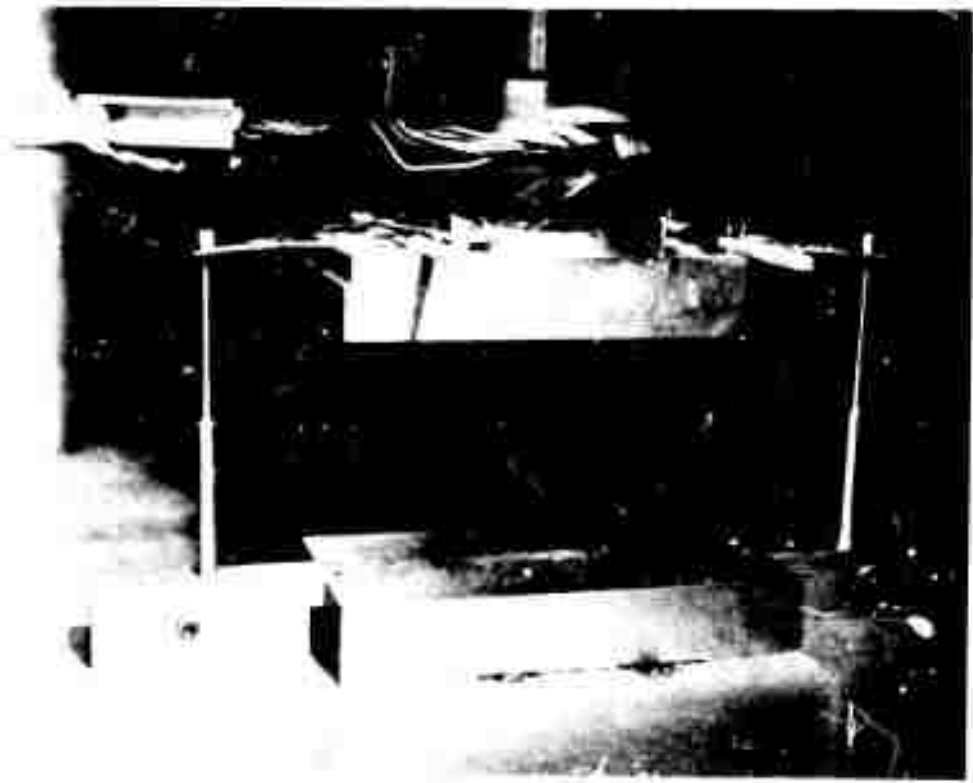


Figure 1.4.2 Vertical Displacement Measurement Device

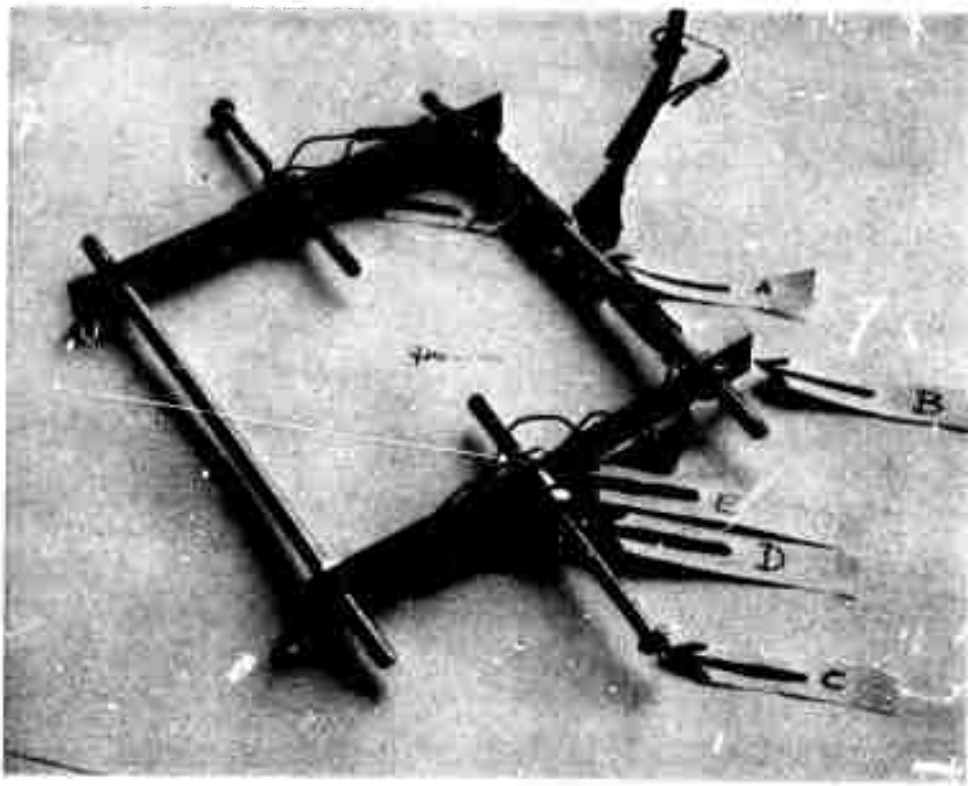


Figure 1.4.3 Horizontal Displacement Measurement Device

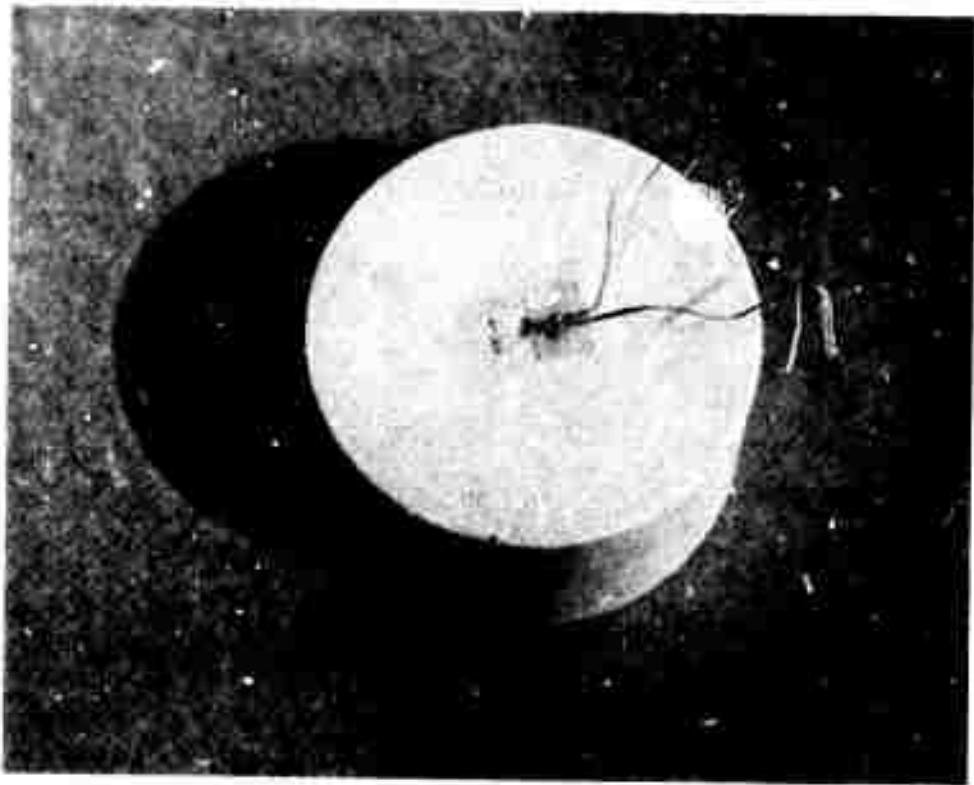


Figure 1.4.4 Brazilian Test Sample

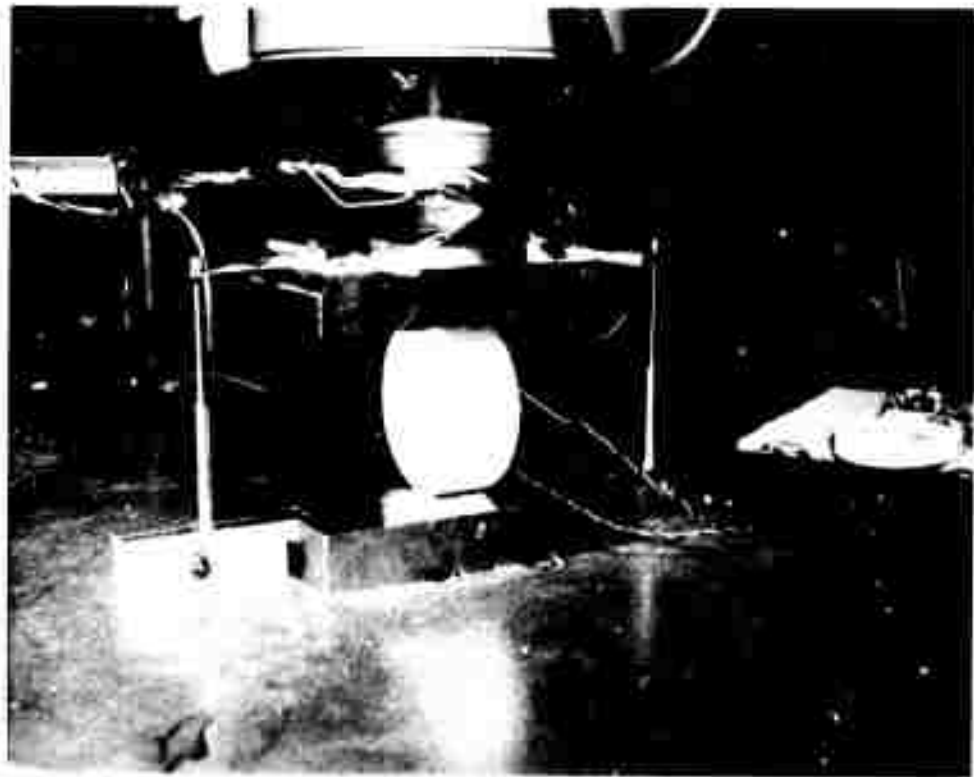


Figure 1.4.5 Brazilian Test

The loading rate in the first phase of the testing program was controlled by the vertical displacement. But we encountered the same problem as Hudson, et al. (4) did. The rock samples broke very violently (shattered to pieces) at the peak load. This, obviously, did not satisfy our objective of obtaining a complete stress-strain curve, and another method of obtaining a complete stress-strain curve must be found. Hudson, et al. were successful in using horizontal strain rate at the center of the disc to control the loading on the sample and to obtain a complete stress-strain curve. Therefore, in this laboratory investigation we also decided to use horizontal strain rate to control the load on the rock sample.

The MB machine, Figure 1. 4. 1, was programmed to reach the highest value of strain allowed by the machine in 800 seconds. The amount of vertical loading exerted by the machine was programmed to be proportional to the horizontal strain rate. If the horizontal strain rate exceeded the preset (programmed) value in the machine, then the vertical load will decrease, and vice-versa. With this servocontrolled machine, it is thought that the change in vertical loading, depending upon the horizontal strain rate, occurs within a few microseconds.

There were, on the average, three samples of each size tested, see Table 1. 4. 1. A typical complete vertical force-vertical displacement plot is shown in Figure 1. 4. 6, and a vertical force-horizontal strain plot is shown in Figure 1. 4. 7.

The testing stopped either when the MB machine went into oscillation* and/or when the strain gages mounted on the sample broke. As the vertical crack along the loaded axis opened up, it also cracked the strain gages securely mounted on the sample, Figures 1. 4. 9, 1. 4. 10 and 1. 4. 11. Approximately half of the tests stopped due to failure of the strain gage. The other half of the tests were terminated when the machine went into oscillations,

*It is believed that the machine went into oscillation when the horizontal strain rate was fluctuating, forcing the closed-loop servocontrolled machine to load and/or unload too rapidly.

TABLE 1.4.1

RESULTS OF BRAZILIAN TESTS ON VALDERS LIMESTONE UNDER HORIZONTAL STRAIN RATE CONTROLLED LOADING

Sample No.	Diameter in inches	Thickness in inches	Peak Load in lbs	Tensile Strength in psi	Average Tensile Strength in psi	% Variation in Tensile Strength	Remarks
35 T	1.009	0.564	1250	1400	1320	6.1	Gages broken, very fine hairline crack, M/C Oscillation
36 T	1.009	0.569	1120	1240			Gages good, very fine hairline crack, M/C Oscillation
27 T	1.009	1.029	1800	1110			Gages broken, sample broken in two halves, (total failure)
28 T	1.011	1.029	2000	1230	1350	25.9	Gages good, very, very fine hairline crack, M/C Oscillation
26 T	1.009	1.040	2800	1700			One gage broken, very, very fine hairline crack
24 T	1.011	2.031	3600	1120			One gage broken, crack extending through the thickness, M/C Oscillation
25 T	1.009	2.036	4500	1400	1350	17.0	Total failure at peak
23 T	1.009	2.062	5000	1530			Total failure at peak
14 T	2.014	0.613	2600	1340			Gage mounting not good, hairline crack
19 T	2.014	0.615	2700	1390	1360	2.2	Total failure
16 T	2.009	0.915	4000	1390			Gages broken, crack extending through thickness
9 T	2.015	0.967	4000	1310			Total failure, crack at 17° with load axis
18 T	2.008	0.975	4200	1370			Total failure, M/C Oscillation
8 T	2.014	1.006	4400	1380			Gages good, very fine hairline crack, M/C Oscillation
15 T	2.009	1.027	4800	1480	1390	7.2	Gages good, very fine hairline crack, M/C Oscillation
17 T	2.009	1.036	4300	1310			Gages good, very fine hairline crack, M/C Oscillation
10 T	2.013	1.042	4900	1490			Gages good, very fine hairline crack, M/C Oscillation

TABLE 1.4.1 (Continued)

Sample No.	Diameter in inches	Thickness in inches	Peak Load in lbs	Tensile Strength in psi	Average Tensile Strength in psi	% Variation in Tensile Strength	Remarks
11 T	2.013	2.021	8300	1300	1310	9.2	Total failure, M/C Oscillation Gages good, very fine hairline crack, M/C Oscillation Gages good, very fine hairline crack, M/C Oscillation
13 T	2.012	7900	1210				
12 T	2.012	9400	1430				
33 T	3.019	0.500	3600	1520	1330	15.0	Total failure at peak Total failure Total failure
32 T	3.018	0.519	3300	1340			
34 T	3.022	0.538	2900	1130			
30 T	3.017	0.932	6300	1260	1410	10.6	Gages good, hairline crack, M/C Oscillation Gages good, fine hairline crack, M/C Oscillation
5 M	3.012	0.975	7100	1540			
31 T	3.020	1.044	7300	1480			
29 T	3.017	1.052	6500	1300	1490	3.5	Total failure just after peak Gages good, very, very fine hairline crack, M/C Oscillation Gage mounting not good, crack extending through thickness
7 M	3.012	1.065	7500	1490			
20 T	3.021	1.951	12900	1390			
22 T	3.019	2.058	14200	1460	1410	3.5	Gages good, fine hairline crack, M/C Oscillation Gages good, fine hairline crack, M/C Oscillation
21 T	3.017	2.061	13600	1390			

Figure 1.4.6 Vertical Force Versus Vertical Displacement, Specimen 34T.

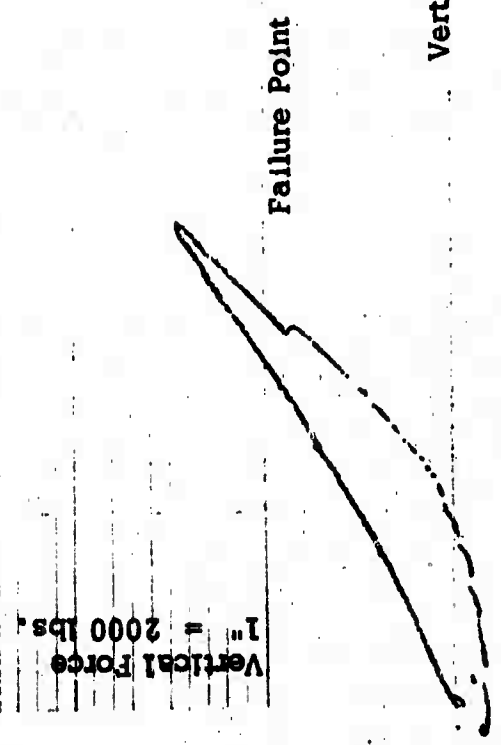
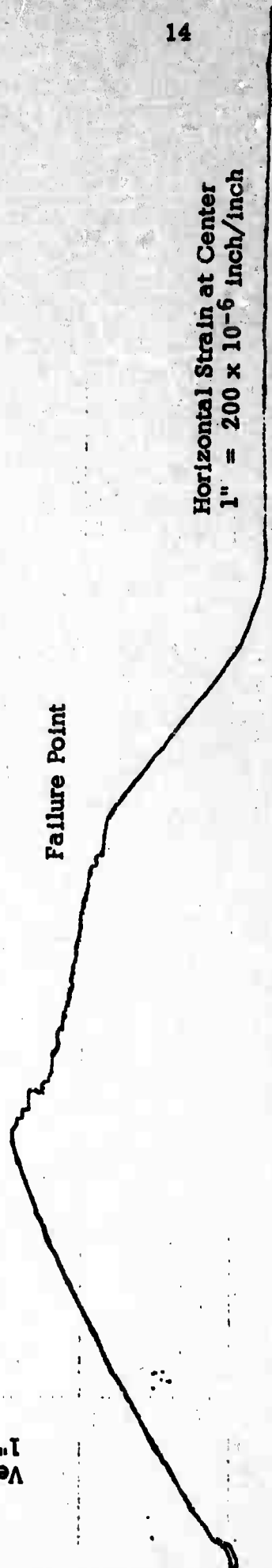


Figure 1.4.7 Vertical Force Versus
Horizontal Strain at the
Center of the Disc,
Specimen 34T.

Vertical Force
1" = 2000 lbs

Failure Point

Horizontal Strain at Center
1" = 200×10^{-6} inch/inch



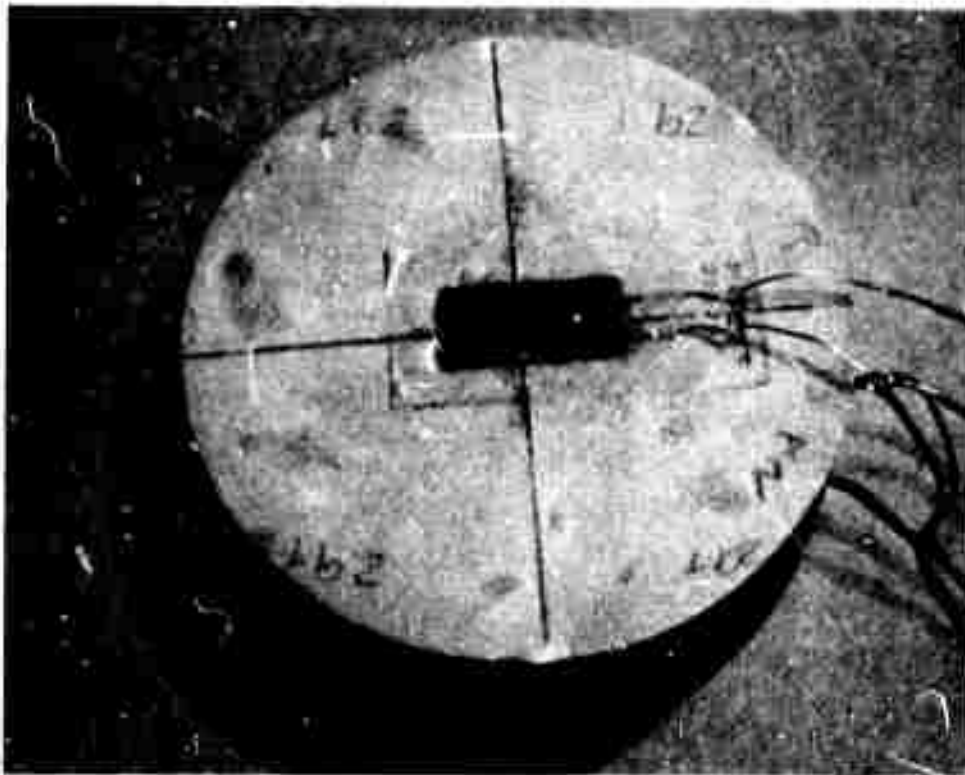


Figure 1.4.8 Sample 29T After Failure

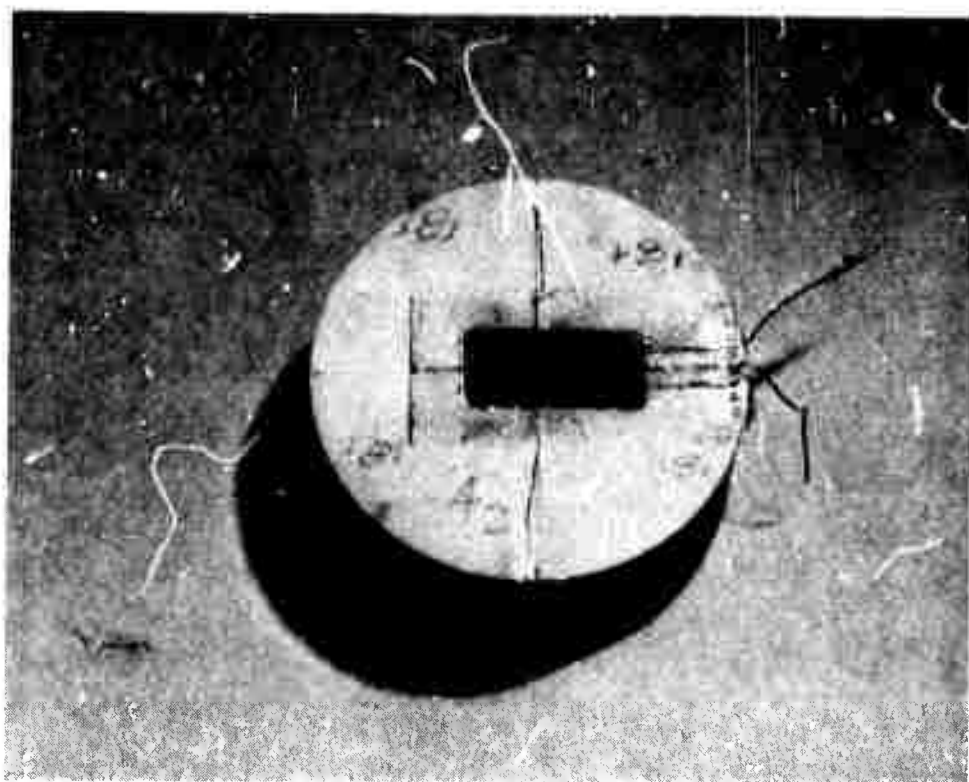


Figure 1.4.9 Sample 18T After Failure

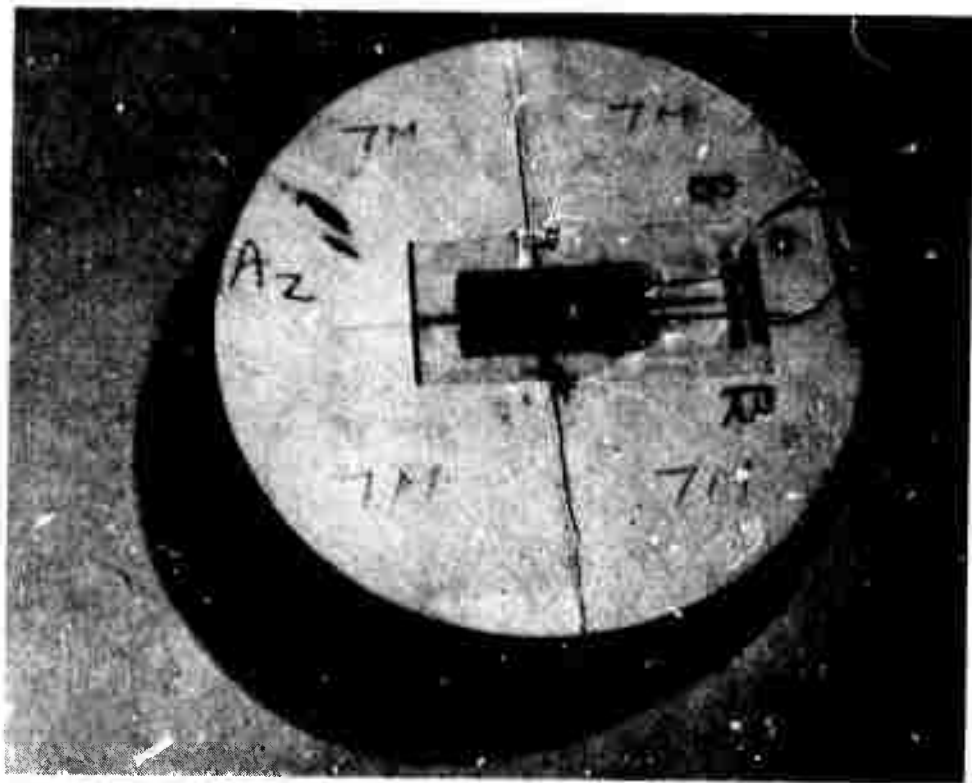


Figure 1.4.10 Sample 7M After Failure

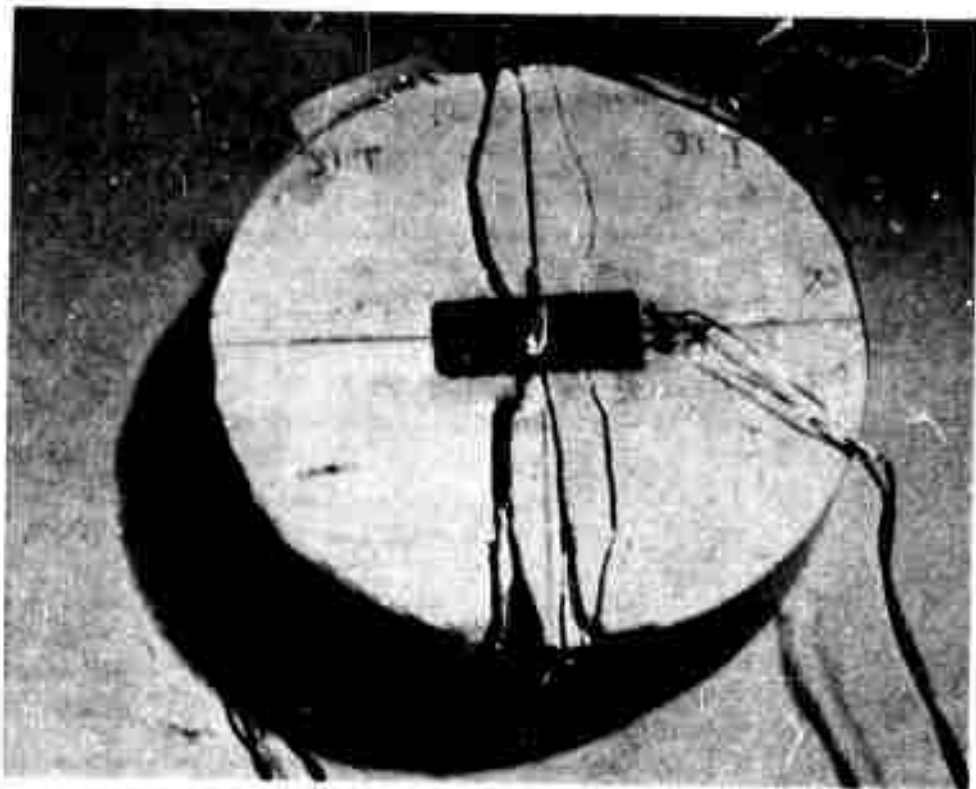


Figure 1.4.11 Sample 31T After Failure

see Table 1. 4. 1. In general, the samples with smaller volume failed due to strain gage failure, Figures 1. 4. 9, 1. 4. 10 and 1. 4. 11, whereas for larger volume samples testing was stopped when the machine went into oscillation, Figure 1. 4. 8. Figures 1. 4. 8, 1. 4. 9, 1. 4. 10 and 1. 4. 11 also show the variation from test to test in the type and amount of fracture. As was expected (1), due to highly localized compressive stress at the point of application of load, the failure crack in general propagated from the outside to the center of the disc along the loaded axis.

1. 5 Discussion of Results

Vertical applied force versus vertical displacement and vertical applied force versus horizontal strain at the center of the disc plots, like Figures 1. 4. 6 and 1. 4. 7, were obtained for all the samples tested. Qualitatively, the plots for all the samples were similar.

After the initial almost linear increase in force versus the displacement for both types of plots, the peak was achieved in about 50 to 80 seconds. The time to reach maximum horizontal strain was set at 800 seconds. For about three to four seconds after the peak was reached, there was no noticeable movement of the plotter pens. At this time, crushing at the load points and the propagation of a hairline crack to the center of the disc was evident. The rock disc did not fail suddenly at this point because the loading was controlled by horizontal strain rate and not by the vertical force or displacement rate. If the loading was controlled by the vertical force or displacement rate, then it is obvious from Figure 1. 4. 6 that the sample would have failed suddenly at the peak load--catastrophic failure. The use of the horizontal strain rate to control the machine prevented the catastrophic failure.

Immediately after the peak point was reached, the crack weakened the sample and reduced the load bearing capacity and the unloading occurred. The sample was still carrying the reduced load, and the horizontal strain in the weakened sample increased (the crack widened). This process continued

until the test was stopped due to breakage of the strain gage, or due to machine oscillations, or when the maximum strain value was reached in the preset total time of 800 seconds.

Table 1. 4. 1 gives some details regarding the Brazilian tests. The mean of the average tensile strength was 1360 psi. Variation in the average tensile strength thus was ± 50 psi or 3.7% around the mean value. From these limited tests, we can then conclude that the sample volume did not have much effect on the tensile strength of the Valders limestone.

Variation in tensile strength within tests was of the higher magnitude, Table 1. 4. 1. For all the one-inch diameter samples, the variation was 16.3%, for two-inch diameter samples it was 6.2%, and for three-inch diameter samples it was 9.7%. The mean of the within-tests variations, for all the samples, was 10.7%. Thus the within-tests variation in tensile strength is significantly higher when compared to the variation in tensile strength due to volume change.

1. 6 Conclusions

From the limited amount of laboratory testing completed so far, the following conclusions may be extrapolated:

1. In order to obtain a complete force-displacement curve for brittle materials, such as Valders limestone, the loading rate must be controlled by horizontal displacement (or strain) rate in order to avoid catastrophic failure at or very near the peak load.
2. The variation in the volume of the samples did not appear to have any significant effect upon the tensile strength of the Valders limestone. The variation in average tensile strength was 3.7% around the mean value.

1.7 Future Program

The general direction of the future program will be as follows:

1. More samples of Valders limestone of each size will be tested, using stress (load) controlled loading for comparative purposes.
2. Two other rock types will be tested, with both strain rate and stress-controlled loading.
3. Statistical methods will be used to aid in evaluation of these results.

Bibliography

1. Timoshenko, S. P., and Goodier, J. N., "Theory of Elasticity," McGraw-Hill Book Company, New York, N. Y., 1951.
2. Coates, D. F., "Rock Mechanics Principles," Mines Branch Monograph 874, Department of Energy, Mines and Resources, Canada, 1970.
3. Fairhurst, C., "On the Validity of Brazilian Test for Brittle Materials," International Journal of Rock Mechanics and Mining Science, Vol. 1, No. 4, 1964.
4. Hudson, J. A., Brown, E. T., and Fairhurst, C., "Optimizing the Control of Rock Failure," Closed Loop, the Magazine of Mechanical Testing, Vol. II, No. 7, by MTS Corporation, Minneapolis, Minnesota.

CHAPTER 2

ONE-DIMENSIONAL MODEL

2.1 Introduction

A one-dimensional progressive failure model is proposed in this chapter. This model consists of linearly elastic springs in parallel. The springs deform independently of each other. They are assumed to be perfectly brittle, i. e., any additional load (force or displacement loading) beyond the peak will cause a sudden failure of the spring. The spring stiffness and strength (failure displacement) values are assigned to the elements by the Monte Carlo technique, using various types of probability distribution functions.

2.2 Distribution Functions

Five types of distribution functions are used to randomly generate the spring stiffness and strength. They are: uniform, left-skewed, right-skewed, unimodal and bimodal. The uniform distribution is well-known, and the others are derived from it as suggested by Hemmerle (1).^{*} These distribution functions are chosen because they represent wide variations and are inexpensive to generate on a digital computer. There is no reason to expect that these distributions represent the properties of a real rock. It is hypothesized that the inhomogeneous real rock properties are statistically inhomogeneous. The varieties of distribution functions should be sufficient to examine their effect upon the progressive failure of the assumed statistically inhomogeneous rock. An added benefit is that the distributions are all bounded over a range, a to b , thus allowing physical interpretation to these bounds. The width of each distribution in terms of variance, V , and mean

* Number in the parenthesis indicates reference number in the bibliography at the end of this chapter.

value of the distribution is tabulated in Table 2. 2. 1.

TABLE 2. 2. 1
STATISTICS FOR THE FIVE DISTRIBUTIONS

No.	Distribution	Subroutine Name*	Mean Value	Width of the Distributions = b-a
1	Uniform	UNIFRM	$\frac{a + b}{2}$	$(12V)^{1/2}$
2	Left-Skewed	RSKEW**	$\frac{2b + a}{3}$	$(18V)^{1/2}$
3	Right-Skewed	LSKEW	$\frac{b + 2a}{3}$	$(18V)^{1/2}$
4	Unimodal	UNIMOD	$\frac{a + b}{2}$	$(24V)^{1/2}$
5	Bimodal	BIMOD	$\frac{a + b}{2}$	$(8V)^{1/2}$

* See Appendix A.

** Subroutine RSKEW actually produces a distribution which is left-skewed, i. e., the mean of the distribution is to the right of the midpoint with the tail of the distribution stretched out to the left. Similarly, LSKEW produces a right-skewed distribution.

We can see from Table 2. 2. 1 that by specifying the mean value and variance, V , we can easily calculate the range of the distribution (values of a and b).

2. 3 Progressive Failure Model

The parallel spring model is loaded with displacement loading. The total stiffness of the model is first computed. It is equal to the sum of stiffnesses of all the springs. After applying the first displacement, we can calculate the force necessary to cause the displacement. It is equal to the total stiffness of the model multiplied by the displacement. This gives us one point for the force versus displacement plot. Before increasing the displacement, a check is made as to whether or not strength (specified in terms

of displacement) of any spring is exceeded. The spring whose strength is equal to the applied load (both in terms of displacement) will fail at the load and is removed from the model. The new total stiffness of the model is computed by subtracting the failed spring stiffness. The displacement is increased, the force needed to cause the displacement is calculated, the failed spring is picked and eliminated, and the cycle is repeated until all springs have progressively failed. All the force versus displacement points are plotted to obtain a force versus displacement plot for the model.

2.4 Discussion of Results

To reduce the number of independent variables in the model and facilitate comparison, a hypothetical rock was selected for modeling in a uniaxial compression test. The specimen is a cylinder with a diameter of two inches and a length of four inches. The rock has a modulus of elasticity of 7.6×10^6 psi, giving total stiffness, $K = \frac{AE}{L}$, of 6×10^6 lb/inch.

The one-dimensional model computer program is given in Appendix A. It was used to obtain force versus displacement plots for the model. There are various independent variables which need to be analyzed. It was decided to analyze the following variables:

- (1) Number of springs
- (2) (a) Strength variance (varied, holding yield point constant),
(b) Strength variance (constant, yield point varied).
- (3) Strength distribution
- (4) Stiffness variance
- (5) Stiffness distribution

The effect of varying number of springs, N , is of two types. The least important but most obvious, Figure 2.4.1, is that the plotting of smaller numbers of points by a "connect the dots" rule will not produce a smooth curve. More important, however, is the statistical "law of large numbers" which says that if "sufficient" number of samples is taken, then the sample

distribution is arbitrarily close to the theoretical distribution. This means that as N approaches infinity, the curve produced by the model becomes realistic. Thus the number of elements should be selected large enough to make the force-displacement curve smooth and reproducible, even with larger number of elements. However, increasing N will increase the cost of analysis, in terms of increased computer time. Figures 2.4.1, 2.4.2, 2.4.3, 2.4.4 and 2.4.5 show the result of varying N ($N = 10, 100, 500$ and 1000) with uniform strength and stiffness distributions. The curves for $N = 500$ and $N = 1000$ are smooth and nearly identical, Figure 2.4.5, while curves for $N = 10$ and $N = 100$ are rough and not reproducible. It was concluded that 500 spring elements were sufficient, and this number was used for subsequent analysis of other variables.

The effect of strength variance on the force-displacement plot may be studied in two different ways: (1) by holding the yield point constant and varying the variance, and (2) by holding the variance constant and varying the yield point.

Let A_s represent the lower bound of the strength distribution. Thus the first element will fail when the applied displacement equals A_s . The model is elastic until the first element fails. Thus, A_s represents the yield point of the model. B_s represents the upper bound of the strength distribution. When the displacement becomes B_s , the last element fails. Thus B_s represents the ultimate failure point of the model.

The result of changing variance of strength distribution, holding A_s ($= 0.004$ inch) constant, is shown in Figure 2.4.6. With $A_s = 0.004$ inch, the model simulates the hypothetical rock which has the yield point of about 24,000 lbs. or 7,600 psi. The strength distribution variance ranged from zero to 5.6×10^{-5} . The stiffness distribution was held constant and both distributions were uniform. With bounded distributions (of the types used here), the role of the strength variance is to fix the upper and lower bounds of the strength distribution if the mean of the distribution is specified. Here, the strength variance was varied holding the lower bound constant at 0.004

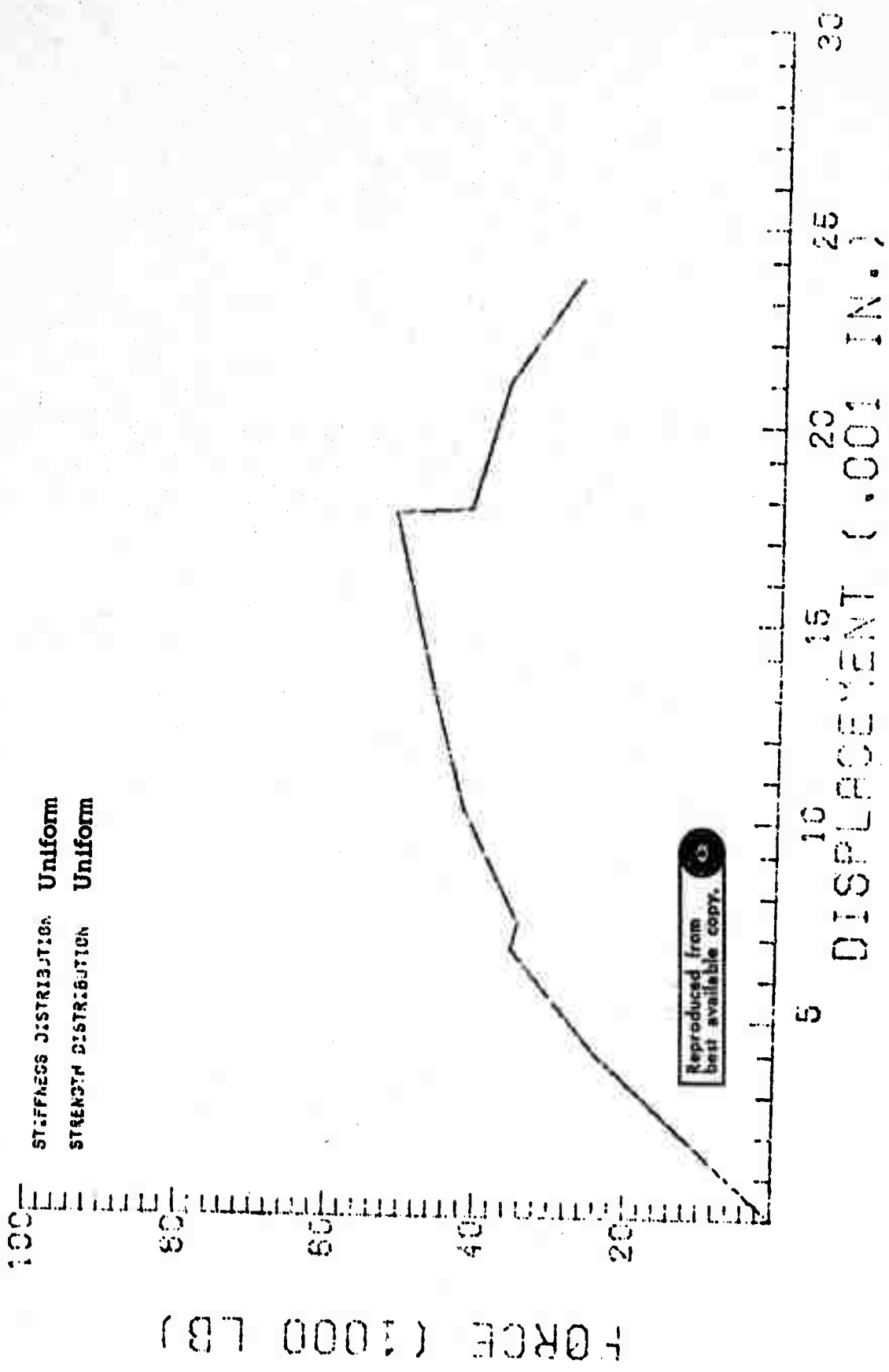


Figure 2.4.1 Effect of N, Number of Spring Elements.
N = 10

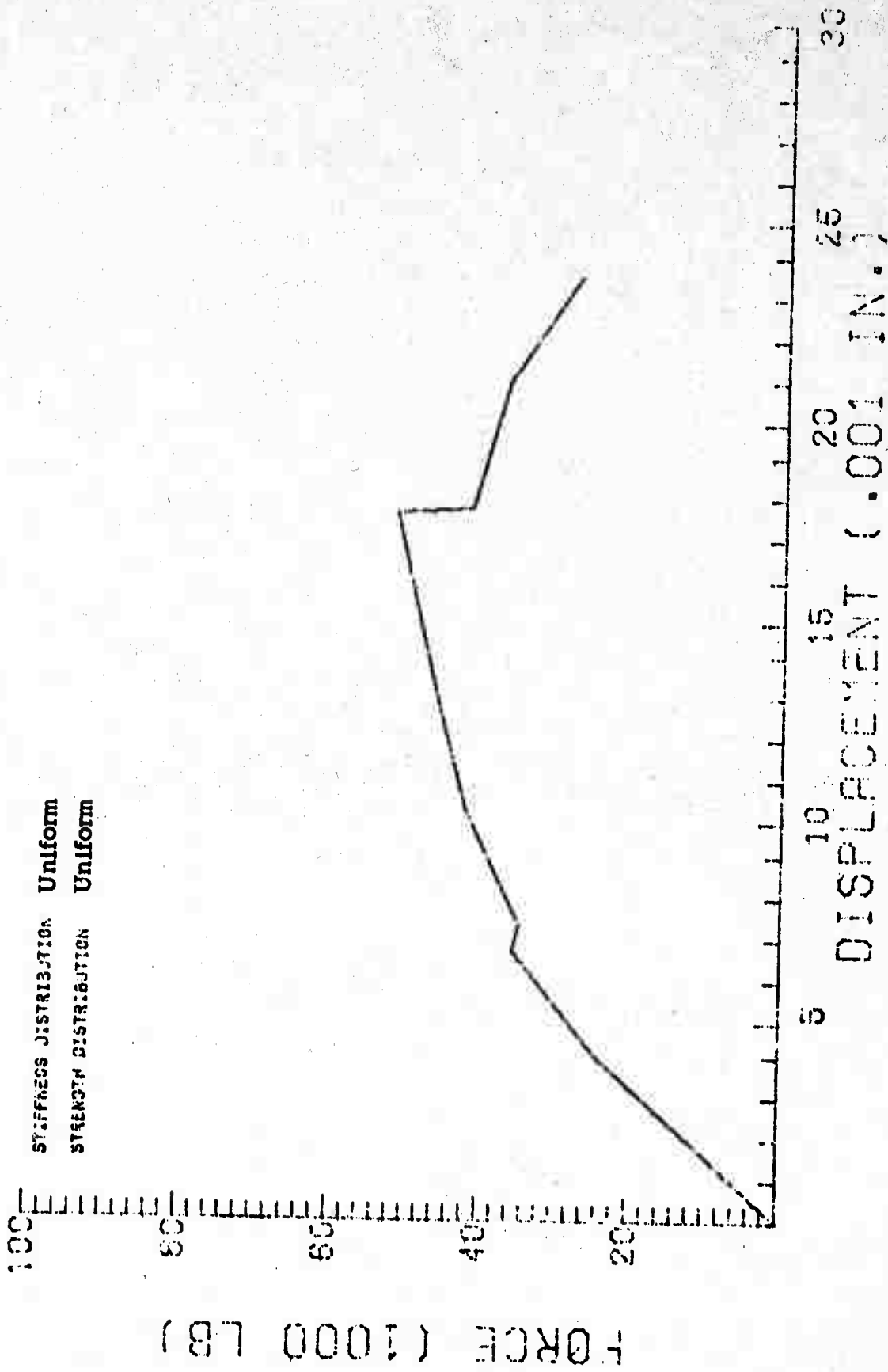


Figure 2.4.1 Effect of N, Number of Spring Elements.
N = 10

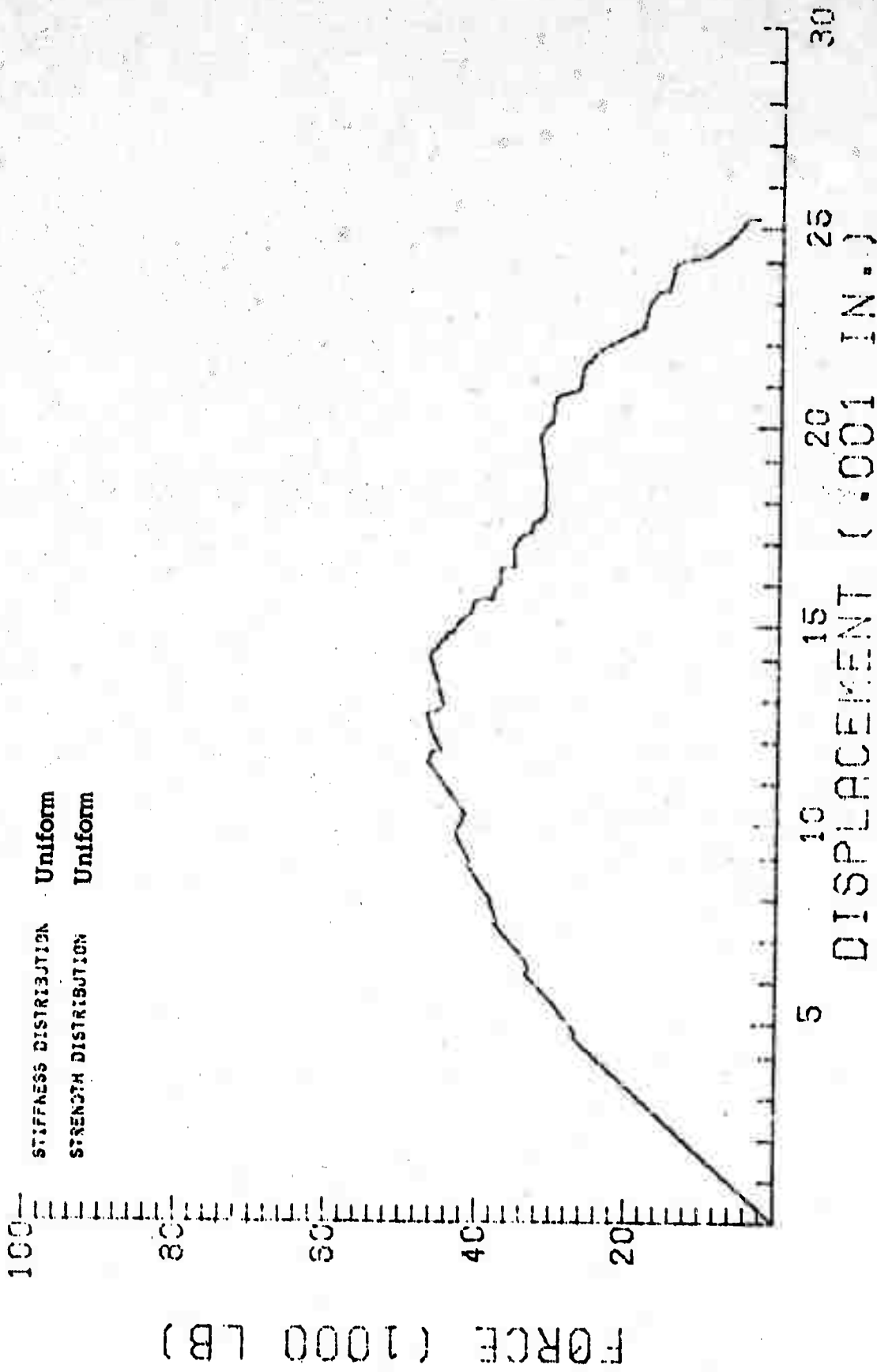


Figure 2.4.2 Effect of N
N = 100

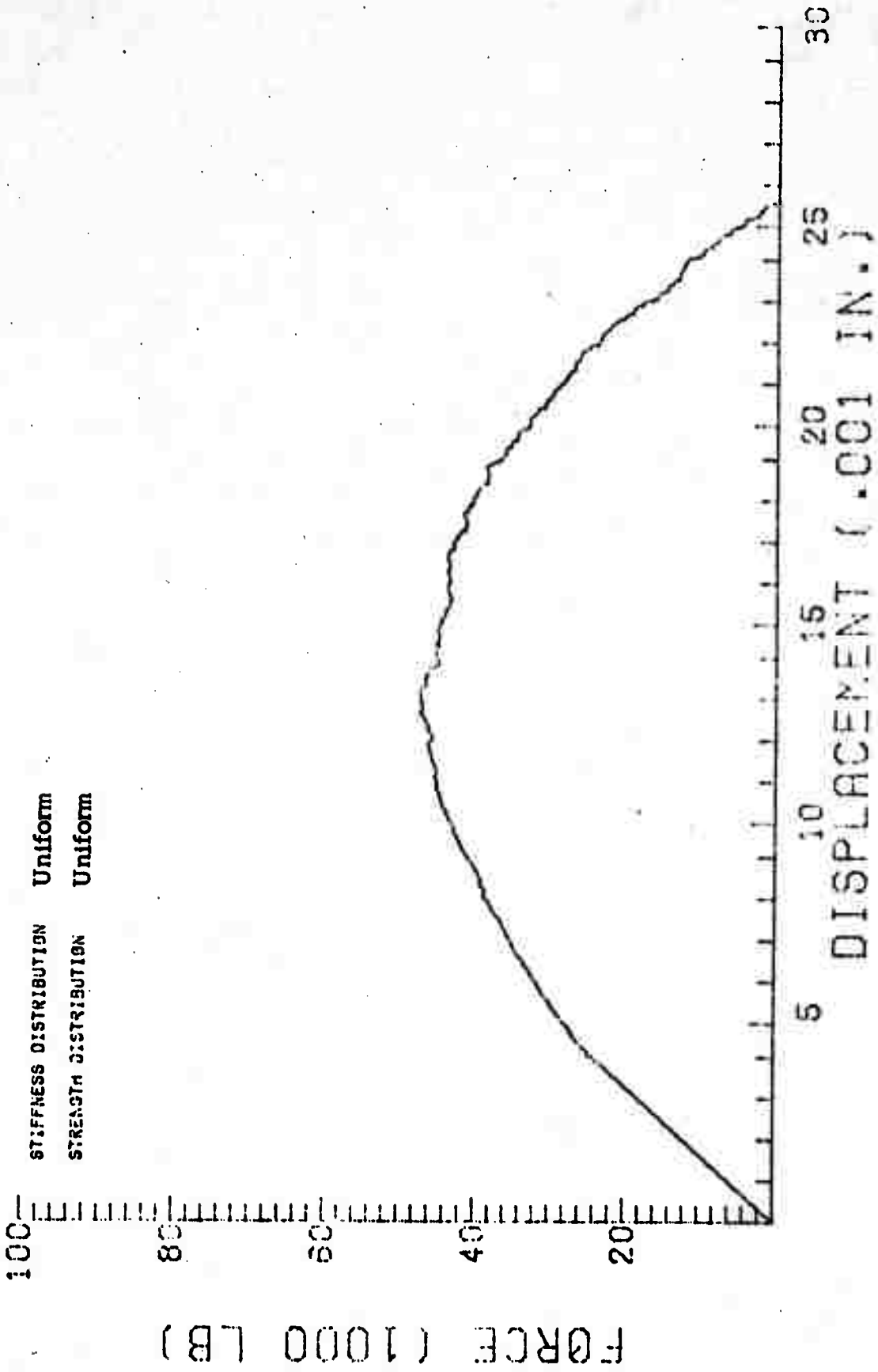
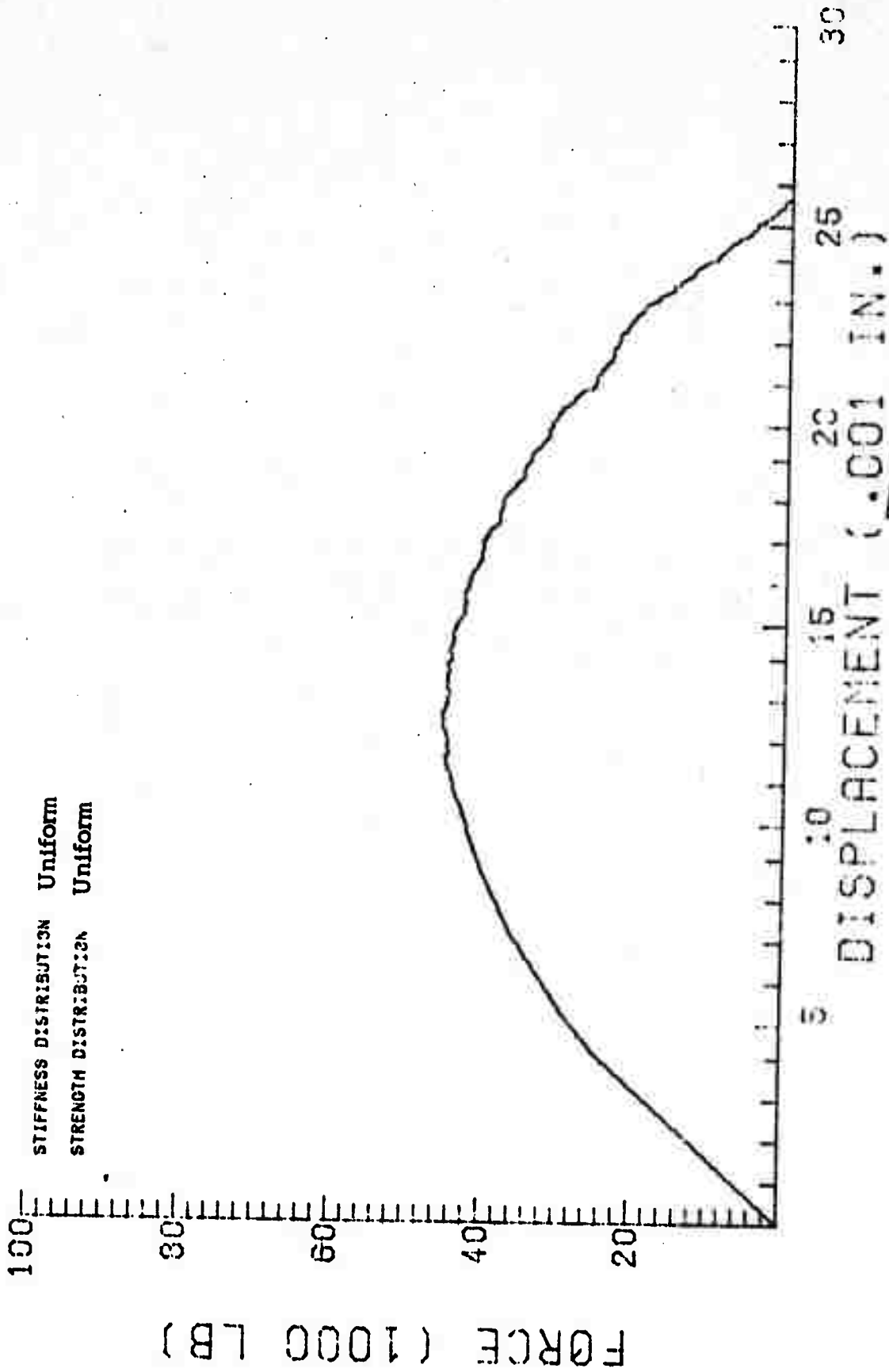


Figure 2.4.3 Effect of N
N = 500



Reproduced from
best available copy.

Figure 2.4.4 Effect of N
N = 1000

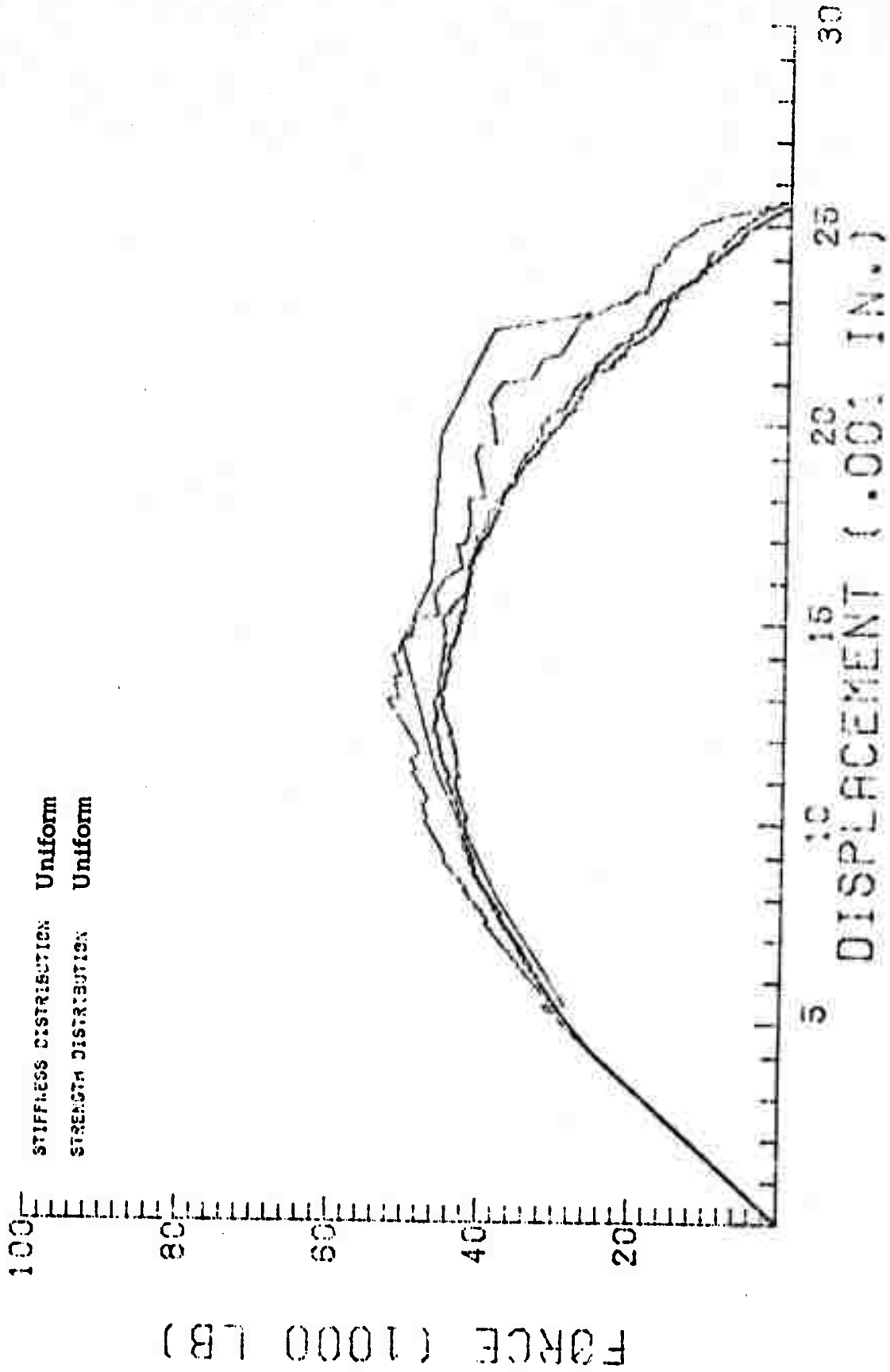


Figure 2.4.5 Effect of N Compared
N = 10, 100, 500, 1000

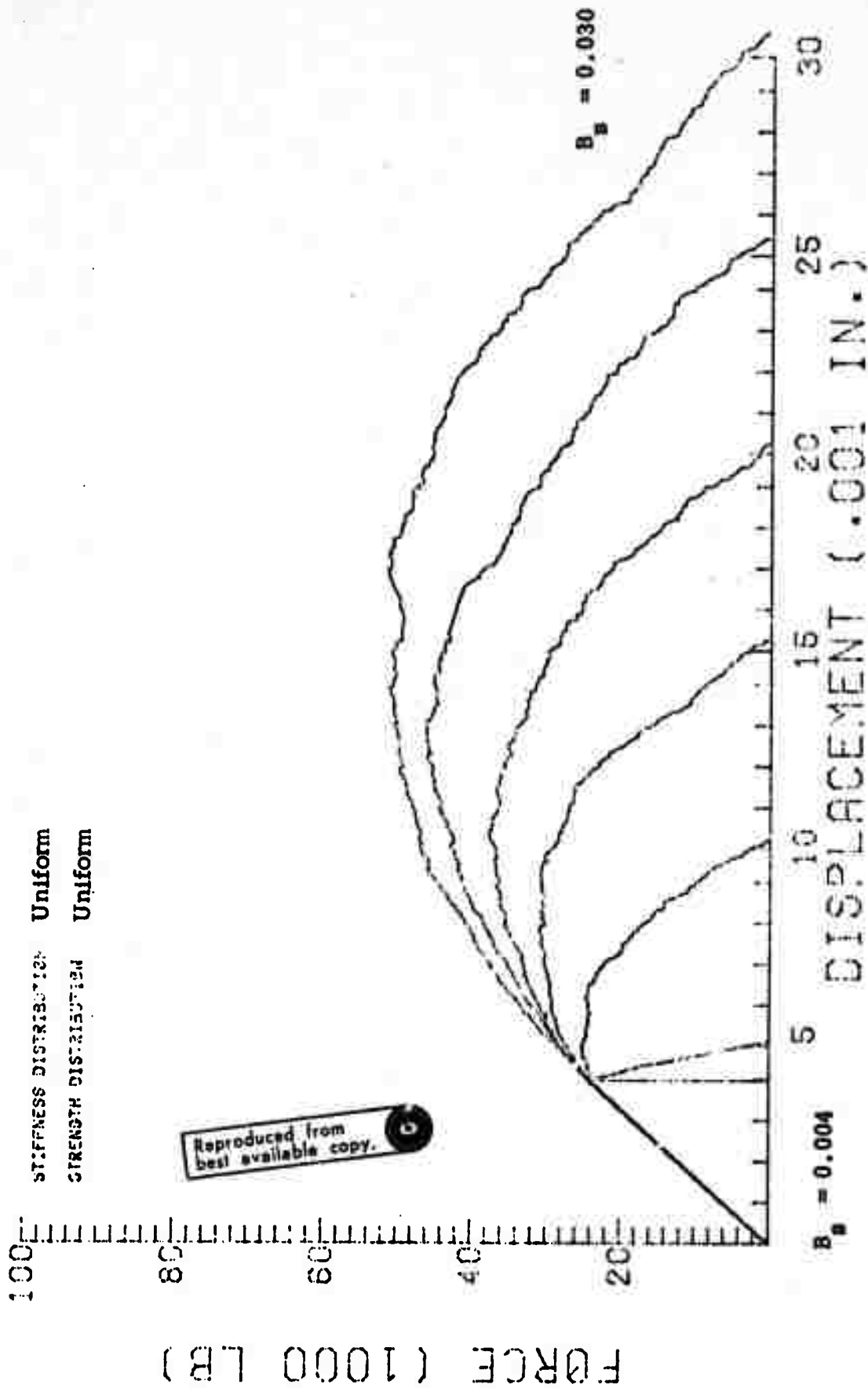


Figure 2.4.6 Effect of B_s , Upper Limit of Strength Distribution.

$B_s = .004, .005, .010,$
 $.015, .020, .025, .030$

$A_s = 0.004$

inch. Thus, the strength distribution fixed the upper bound or the maximum displacement at which the specimen will fail. If A_s and B_s are coincident, variance = 0, then the yield, peak and maximum displacement occur at the same displacement and weakest link failure occurs. This implies that the hypothetical rock simulated has a homogeneous strength.

The second way to study the effect of rock strength variance is to vary the yield point of the rock, but holding the variance constant. The strength and stiffness variance was held constant and the uniform distribution was used. A_s varied from 0 to 0.008 inch. The resulting force-displacement plots are shown in Figure 2.4.7.

From Figures 2.4.6 and 2.4.7, we can readily see that the effect of the strength variance on the force-displacement plot is significant.

Figures 2.4.8 to 2.4.12 show the effect of the five strength distributions on the force-displacement plots. The strength distributions are uniform, unimodal, left-skewed, right-skewed and bimodal, respectively. The uniform stiffness distribution was held constant. The strength and stiffness variance and yield point were also held constant. We can see that the strength distributions have marked effect upon the force-displacement response of the model.

Effect of stiffness variance is shown in Figure 2.4.13. The strength variance and the yield point, A_s , were held constant. The stiffness variance ranged from zero to ten with the mean stiffness fixed at $6 \times 10^6/N$, where N is the total number of spring elements. The uniform distribution was used for the strength and the stiffness variance. We can see from Figure 2.4.13 that the stiffness variance does not have a very significant effect upon the force-displacement response of the model.

Figure 2.4.14 shows the effect of the five stiffness distributions on the force-displacement plots. The stiffness distributions are uniform, unimodal, left-skewed, right-skewed and bimodal, respectively. The uniform strength distribution was held constant. The strength and the stiffness

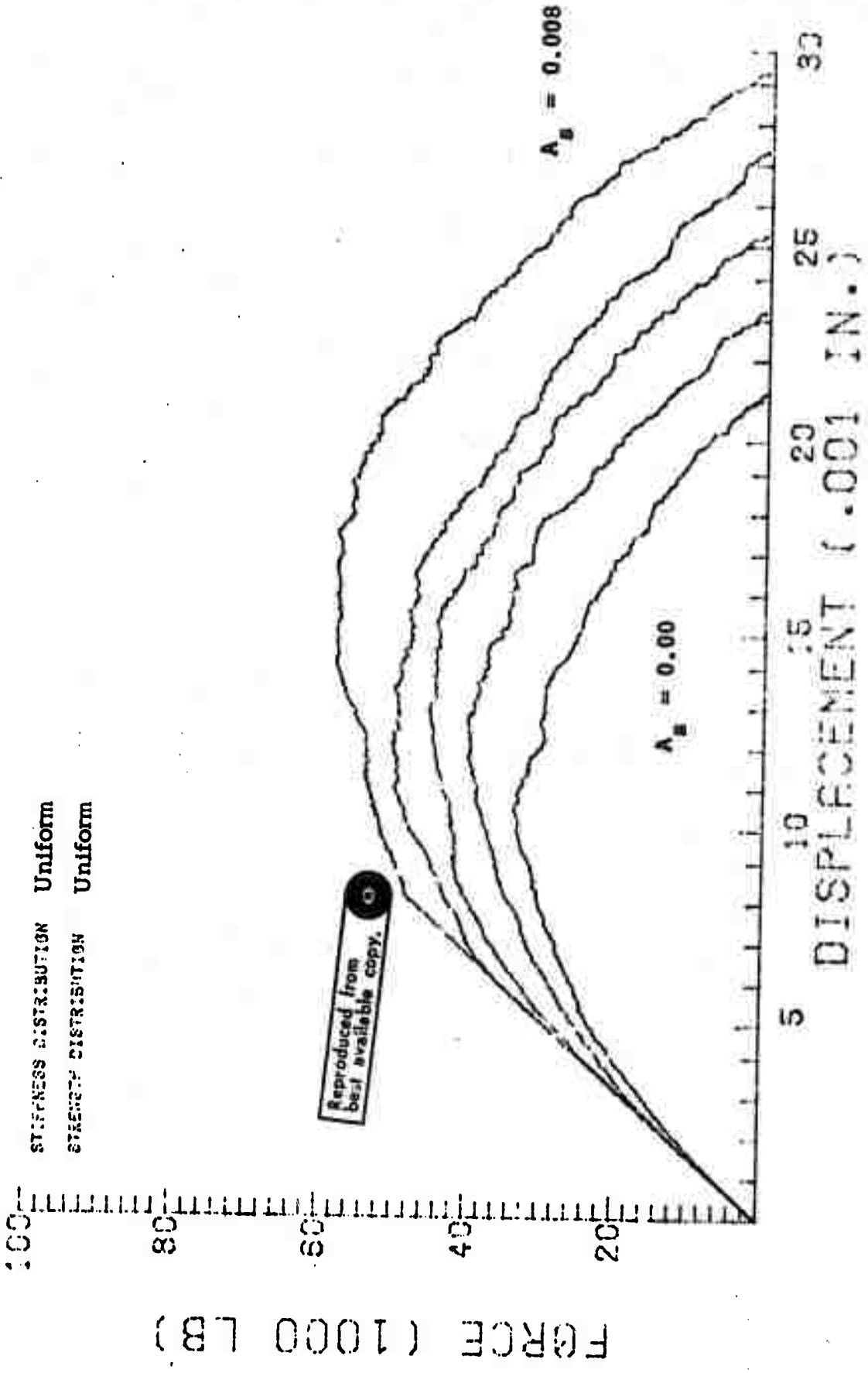
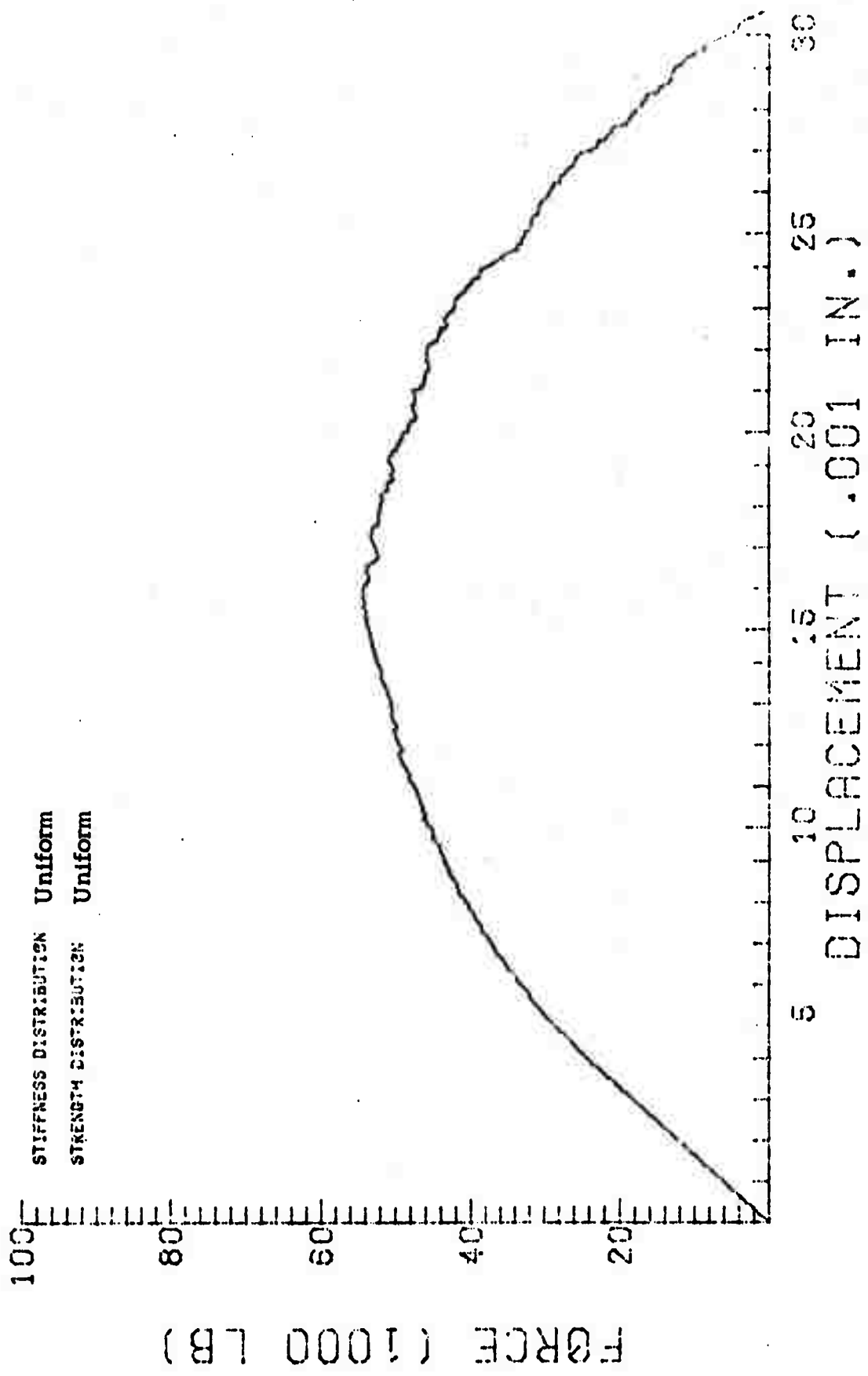


Figure 2.4.7 Effect of A_B , Lower Limit of Strength Distribution.
 $A_S = 0.00, .002, .004, .006, .008$



STIFFNESS DISTRIBUTION Uniform
STRENGTH DISTRIBUTION Uniform

Figure 2.4.8 Strength Distribution: Uniform

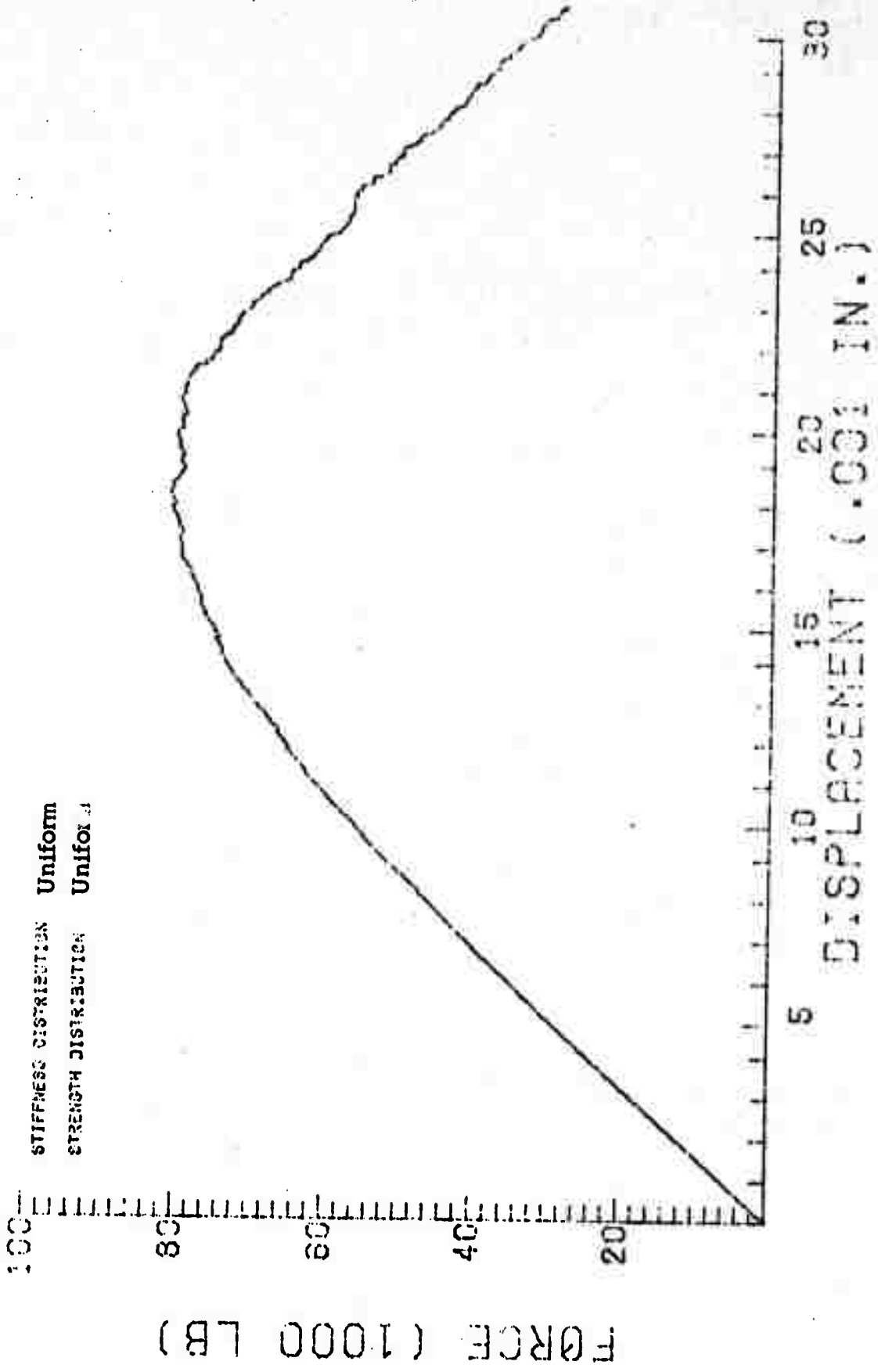


Figure 2.4.9 Strength Distribution Unimodal

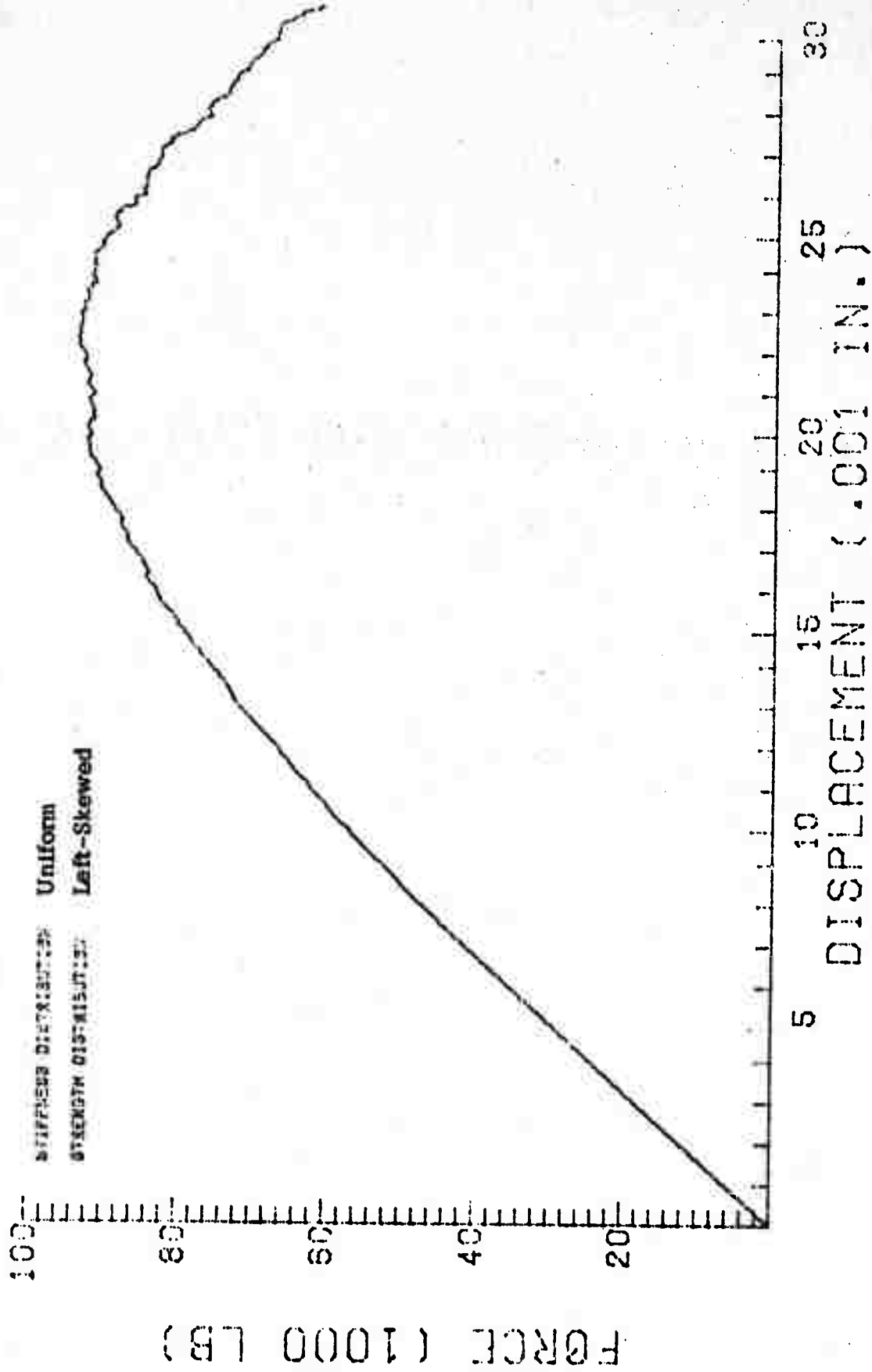


Figure 2.4.10 Strength Distribution Left-Skewed

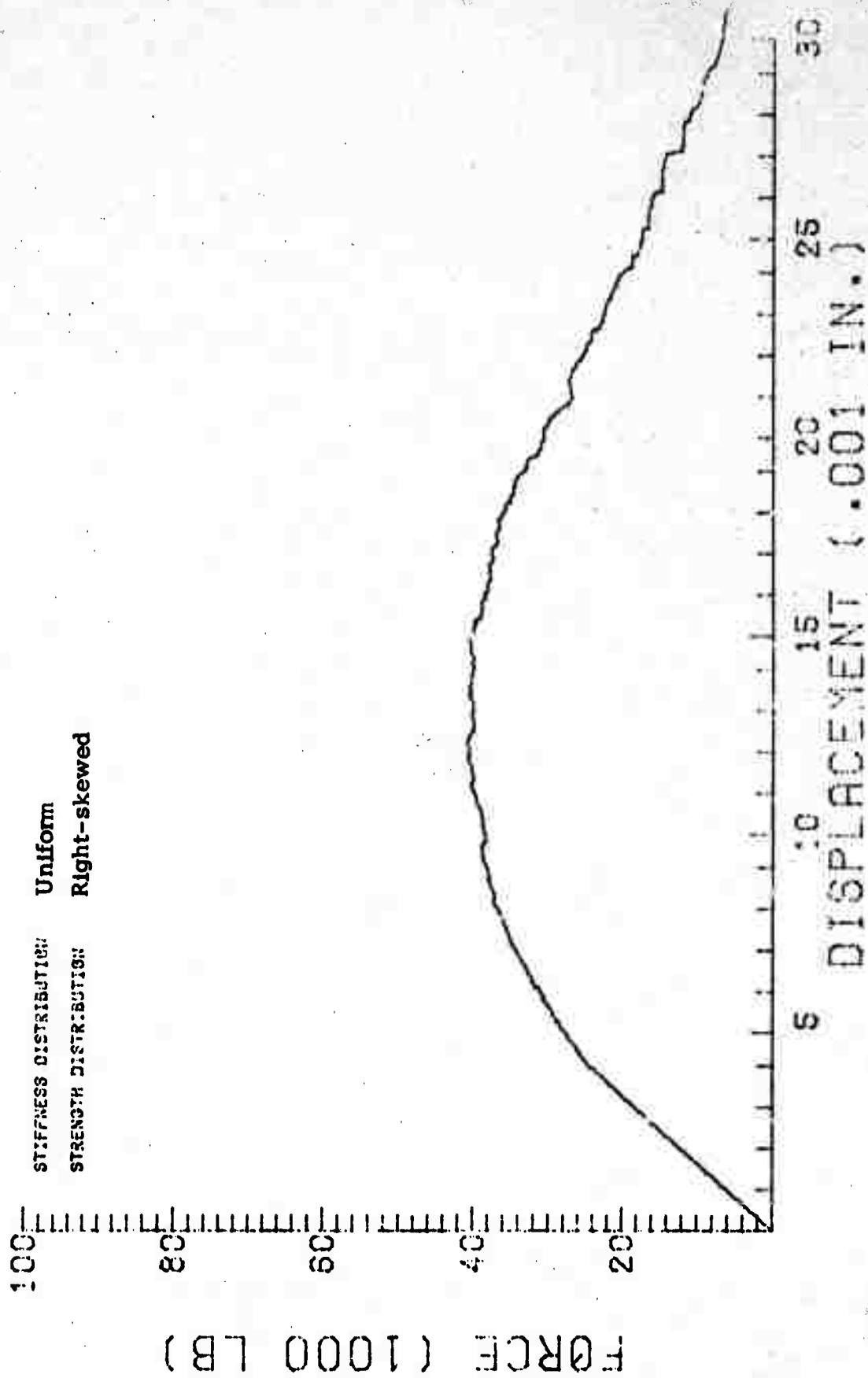


Figure 2.4.11 Strength Distribution Right-Skewed

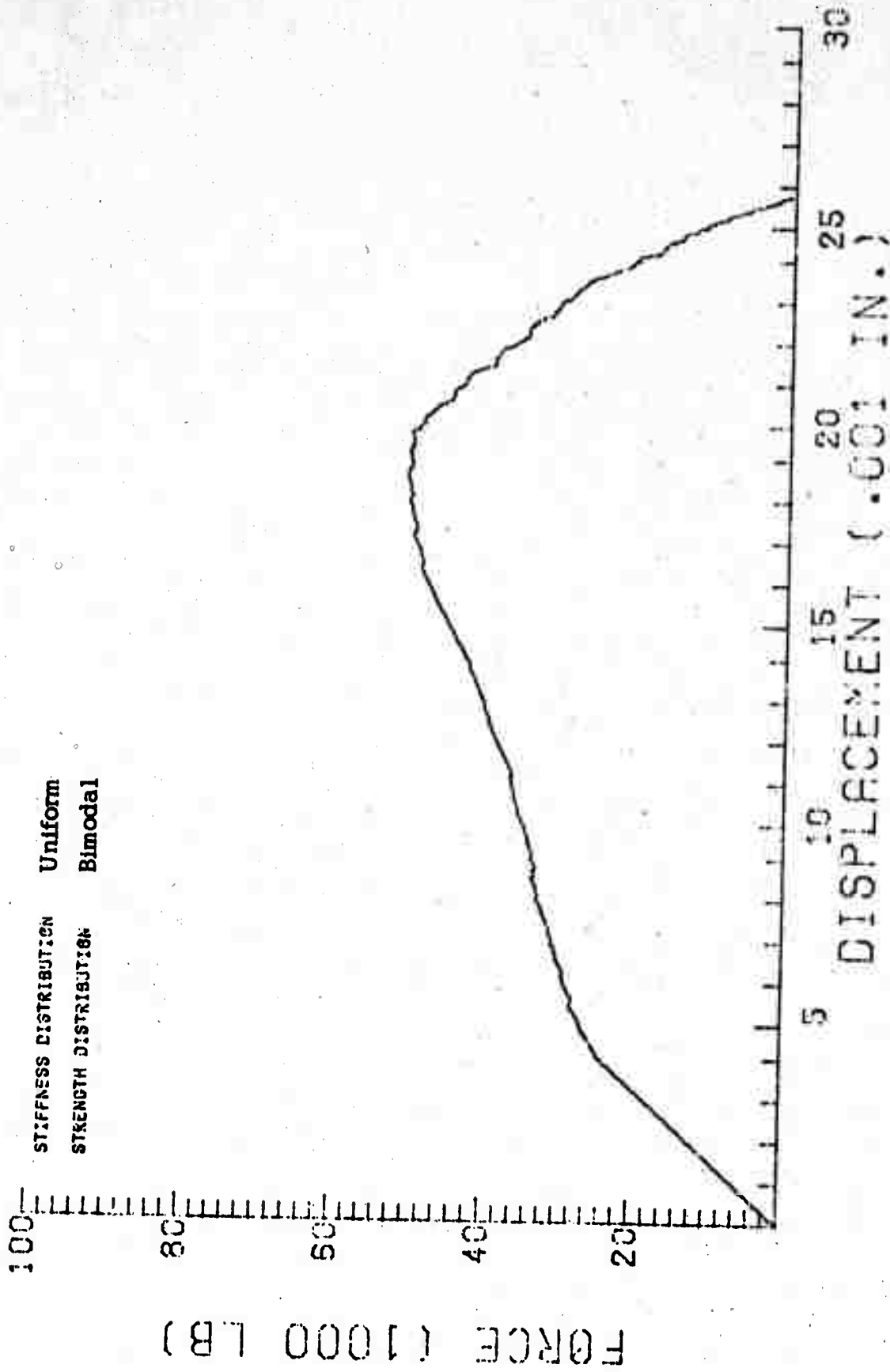


Figure 2.4.12 Strength Distribution Bimodal

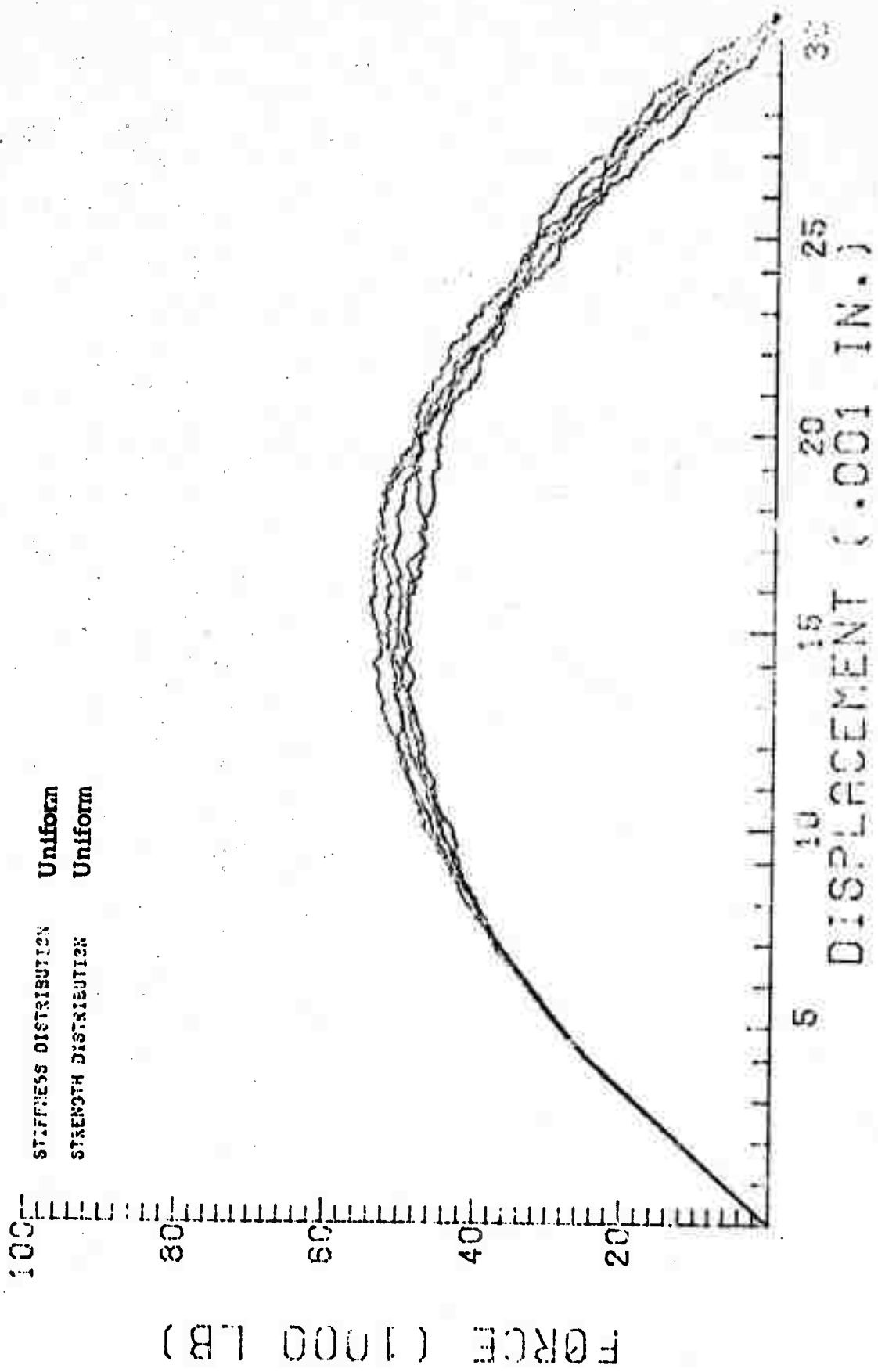
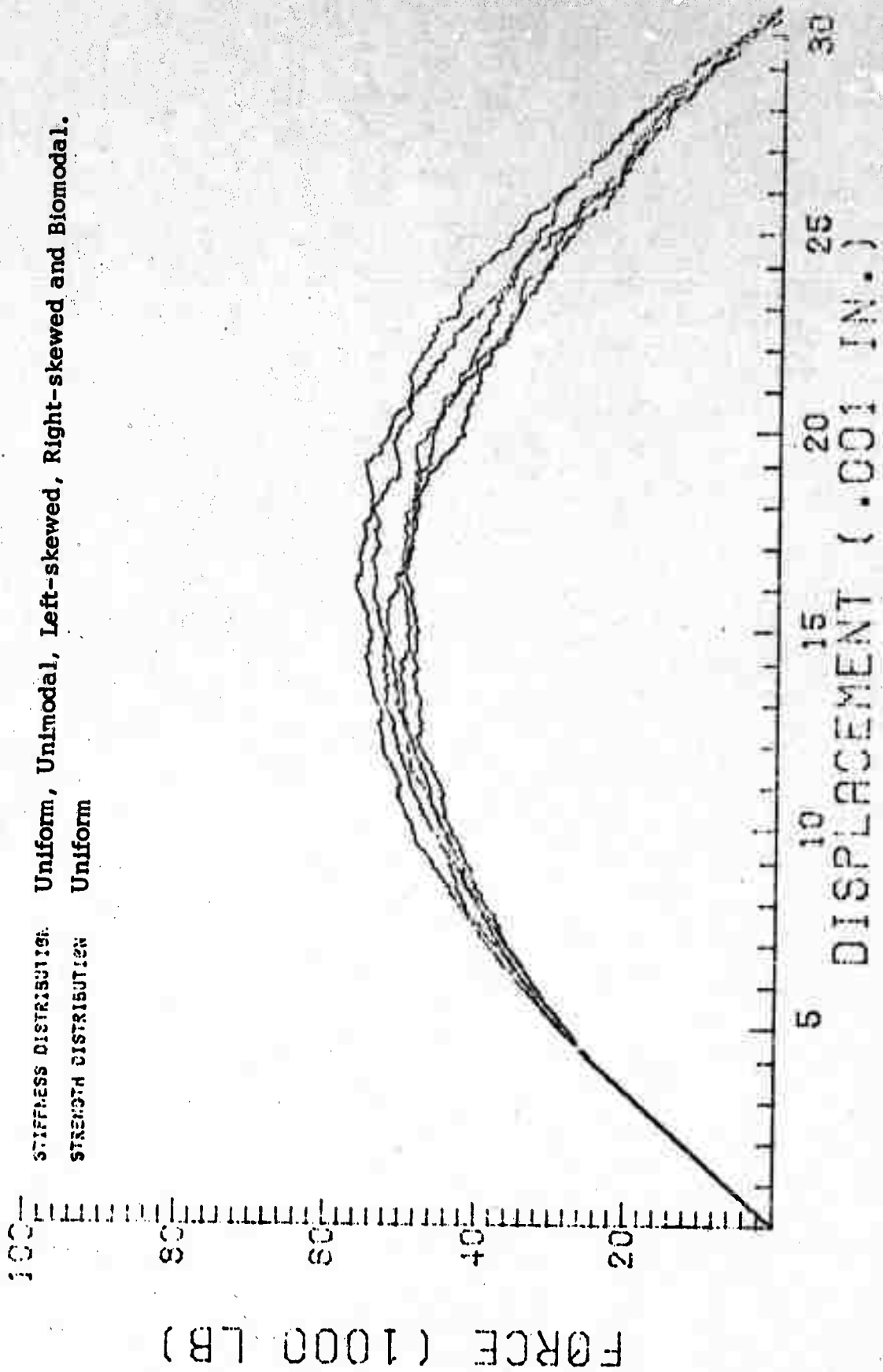


Figure 2.4.13 Effect of V_K , Stiffness Variance.



STIFFNESS DISTRIBUTION: Uniform, Unimodal, Left-skewed, Right-skewed and Biomodal.
STRENGTH DISTRIBUTION: Uniform

Figure 2.4.14 Effect of varying stiffness distribution.

variance and the yield point were also held constant. We can observe from Figure 2. 4. 14 that the stiffness distributions do not have a very significant effect upon the force-displacement response of the model.

2. 5 Observations

The following observations may be made regarding the one-dimensional model.

- (1) The model does not have any direct use in practice, but it serves a very important use in this study. It serves as a simple model to study numerous variables involved. This will help a great deal in the development of two and three-dimensional model.
- (2) This simple one-dimensional model is relatively very inexpensive to use in terms of computer time for analysis of variables. We can expect a similar effect of variables in case of two- and three-dimensional model, thus eliminating a need for detailed analysis of these variables in subsequent model developments.
- (3) The use of bounded distributions allow the effect of variables to be examined with physical interpretations to be placed on these bounds.
- (4) Five hundred spring elements are sufficient for this model to obtain smooth force-displacement plots.
- (5) The minimum value of strength distribution defines the yield point for the model and the maximum value defines the ultimate failure displacement.
- (6) The shape of the strength distribution has a marked effect upon the force-displacement plot of the model.
- (7) The stiffness variance and the shape of the stiffness distribution does not have a very significant effect upon the force-displacement plot of the model.

Bibliography

1. Hemmerle, W. J., "Statistical Computations on a Digital Computer," Blaisdell Publishing Co., 1967.
2. Madison Academic Computing Center, Plotting Routines Summary, Plotting Routines Series, MACC, October 1970.
3. Madison Academic Computing Center, Random Number Routines, Mathematical Routines Series, MACC, October 1969.

CHAPTER 3

TWO-DIMENSIONAL MODEL

3.1 Introduction

While many papers exist on the subject of inhomogeneity in elastic and plastic problems, they treat mainly that class of problems which we have called deterministically inhomogeneous. What we have called statistical inhomogeneity--which is a more realistic model for polycrystalline materials such as rock--cannot be treated by exact methods. Neither can they be easily handled by finite difference methods, due to the difficulty with boundary conditions between regions with different properties.

The emergence over the last decade of the finite element method has no less than revolutionized all of continuum mechanics. Problems that were previously considered intractable or at least very difficult, are now solved routinely. The method has also seen much use in rock mechanics as witnessed by increased volume of papers.

Inhomogeneous problems of all kinds have been especially simplified by the finite element method. Each element can be assigned its own unique properties with no more difficulty than assigning the same property to all elements.

This approach was used by Su, Wang, and Stefanko (1)* to study the stress distribution around a mine opening (circular tunnel). They assumed that both Young's modulus and Poisson's ratio were normally distributed. Not surprisingly, in light of the "law of large numbers," they found that the mean of the stress distribution for any region approached the value it would have if the material was assumed homogeneous but that large differences in local stresses would occur when compared to the material being normally distributed elastic properties.

* Number in the parenthesis indicates reference number in the bibliography at the end of this chapter.

All other papers encountered in a literature search referred to deterministic inhomogeneity which is, of course, easily treated by the method.

It will be assumed that the reader is familiar with the finite element method. Many excellent references and textbooks are available.

3.2 The Model

A finite element progressive failure model was developed and programmed in FORTRAN for solution by a digital computer. While some portions of existing programs from several sources (2) were used, it was found that no existing program could be satisfactorily modified. The majority of work under the present contract has, therefore, been devoted to writing the program given in Appendix B.

Basically, the model consists of a series of elastic analyses on a two-dimensional finite element structure. In each cycle the element is found which has the worst combination of principal stress (computed from the elastic analysis) and strength (assigned as an element property in the program). This element is then considered "failed" by the program. This maximum principal stress criterion of failure is clearly an oversimplification of elemental failure mechanism for rock. Since such failure mechanisms are the subject of heated debate among experts in fracture mechanics, the principal stress criterion may be considered an initial step toward an eventual more realistic model.

From the ratio of the maximum or minimum principal stress in the critical element to its compressive or tensile strength, the loads and displacements are scaled so that the element is exactly failed, i. e., the ratio becomes one. The program then computes the force needed to cause the calculated displacement and reports the number of the failed elements, the external load causing the failure, and the displacement under the load. Any other force or displacement quantities needed can be printed out at the same time.

Most of the element stiffness is removed by subtracting 99% of the element stiffness of the failed element. Not subtracting the entire stiffness avoids division by zero in the matrix solution process. The idea of assuming the failed element to lose almost all of its stiffness again is an oversimplification and should again be considered but an initial step.

The initial force and displacement conditions are reset and the cycle is repeated as an elastic analysis of the remaining (unfailed) portion of the structure.

It should be noted that the program is not iterative in the usual sense, i. e., it does not increment or monotonically increase the load (neither force or displacement load). The elastic analysis is iterated. In each cycle, a new structure is analyzed. The new structure essentially omits (except for 1%) the element failed in the previous cycle. The cycles are continued until complete failure occurs.

3.3 Test of the Model

For initial testing of the finite element progressive failure model, the diametral compression or Brazilian test was chosen. It suits this purpose very well since it includes both tensile and compressive stress regions.

The Brazilian test is accepted to be an indirect tensile strength test for rock, and a rather large proportion of reported tensile strengths for rocks are obtained by this method. Recent investigations (3) have shown that failure rarely, if ever, initiates at the tensile stressed region in the center of the loaded diameter. This was also confirmed by the laboratory investigation outlined in Chapter 1. Failure is initiated by crushing under the loads at the ends of the diameter and immediately proceeds inward, creating the vertical crack commonly seen. The compressive stress at the ends of the diameter is theoretically infinite under a line load but decreases as the arc of contact is increased. Fairhurst (4) showed that tensile failure is theoretically possible if the compressive strength/tensile strength ratio was greater

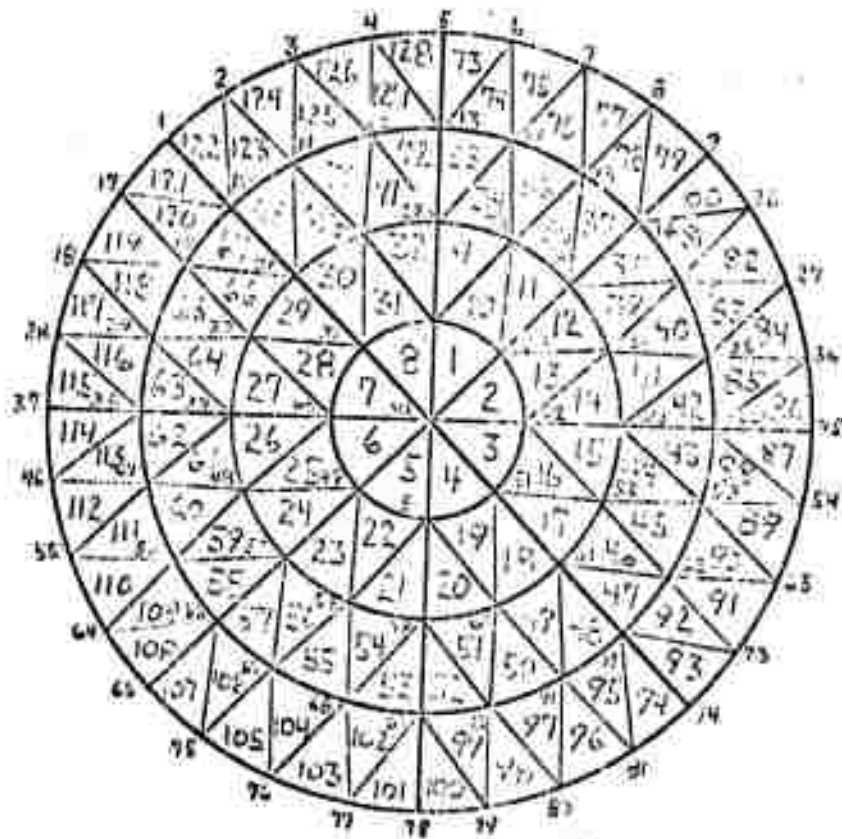
than about 12 for an arc of contact $\alpha = \tan^{-1} 1/12$, but that for $\alpha = \tan^{-1} 1/6$ tensile failure is possible with a ratio of 8. (Note: $\tan^{-1} 1/12$ is about 4.8° and $\tan^{-1} 1/6$ is about 9.6° .) Hudson, et al. (3) found that even for arcs of contact exceeding 10° , no tensile failure of the assumed kind could be found.

A finite element mesh to model the Brazilian test is shown in Figure 3.3.1. It consists of 81 nodes comprising 128 triangular elements. A structure with five rings of elements (121 nodes, 200 elements) was also tried but could not be run due to computer size limitations.

Constant strain triangles are also probably preferable to more sophisticated elements. At least they will be easier to work with. The program size is limited by the computer core size and determined primarily by the size of the stiffness matrix. For a two-dimensional structure, this size is twice the total number of nodes. Constant strain triangles can be shown to give the largest number of elements for a given degree of accuracy of results and thus for a given program size they provide the maximum information about the progression of failure. The node numbering scheme shown gives a bandwidth of 36, which is felt to be a minimum for the four ring structure.

The results of six computer runs are presented in the next section. For five of these runs, the specimen was loaded by a vertical downward displacement on node number five while the opposite node (number 78) was held fixed in both directions. This simulates not a live load but an arc of contact of $11-1/4^\circ$ (one-half element width in each direction). Because the high stress gradients under the load cannot be well modeled by the constant strain triangles, this probably corresponds to a somewhat smaller arc on real rock. One test (A-3) had three nodes loaded and three fixed simulating an arc of contact of $33-3/4^\circ$.

The first three runs were with homogeneous element properties. The fourth and fifth runs were with element strengths distributed two different ways, and the sixth run had only element Young's modulus distributed. Poisson's ratio was held constant at 0.25, but would be varied in later testing.



Reproduced from
best available copy.

Figure 3.3.1 Brazilian Test Finite Element Mesh

Properties were assigned to each element by subroutine CARDS using the Monte Carlo scheme developed for the one-dimensional model. Only the uniform distribution was used but the other distributions may also be tried. It is doubtful that they will make any large difference in the results.

Compressive strength for any element is a constant multiple (provided as data) of the stochastically generated tensile strength. Since any element can fail only once, this does not disturb the randomness of the strengths.

3.4 Test Results

The conditions of the six tests are shown in Table 3.4.1. The Young's modulus was a constant 7,600,000 psi except in test A-6 where its mean was 7.6×10^6 psi. The mean (or constant) tensile strength was chosen to give a mean compressive strength of 13,000 psi.

Let us discuss the results for each test individually.

In test A-1, the specimen failed immediately by crushing the elements adjacent to the loaded node. With these elements failed on both ends of the loaded diameter, there was little resistance to large displacement and the test was terminated. This test points up a particular inadequacy of the model in that all load resistance would not be removed by crushout under the loads in a real specimen. The crushed zone would retain considerable stiffness and a crack would propagate from the outside to the center of the specimen. The failure initiation of the model appears entirely correct, however.

With a higher ratio of compressive to tensile strength in test A-2, failure initiated at the center of the disc and ran outward. The progression of the failure is shown in Figure 3.4.1. Ultimate failure was by crushing under the loads as before, but initiation and propagation were as expected for the higher ratio of tensile to compressive strength. Force-displacement under the load for test A-2 is shown in Figure 3.4.2. It is easily seen that either force or displacement controlled loading will produce complete failure simultaneously with failure initiation. After $n = 11$, the specimen has failed

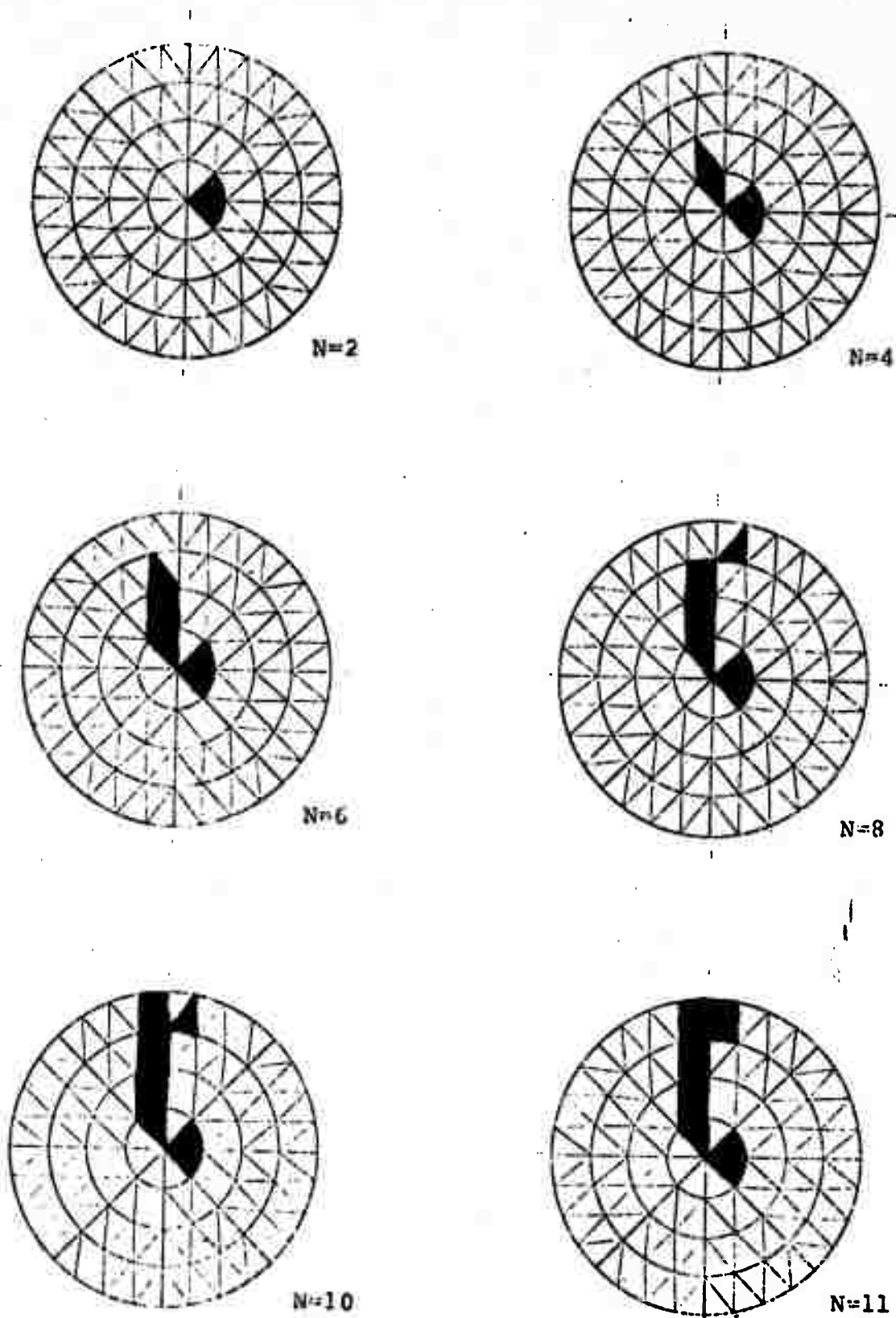
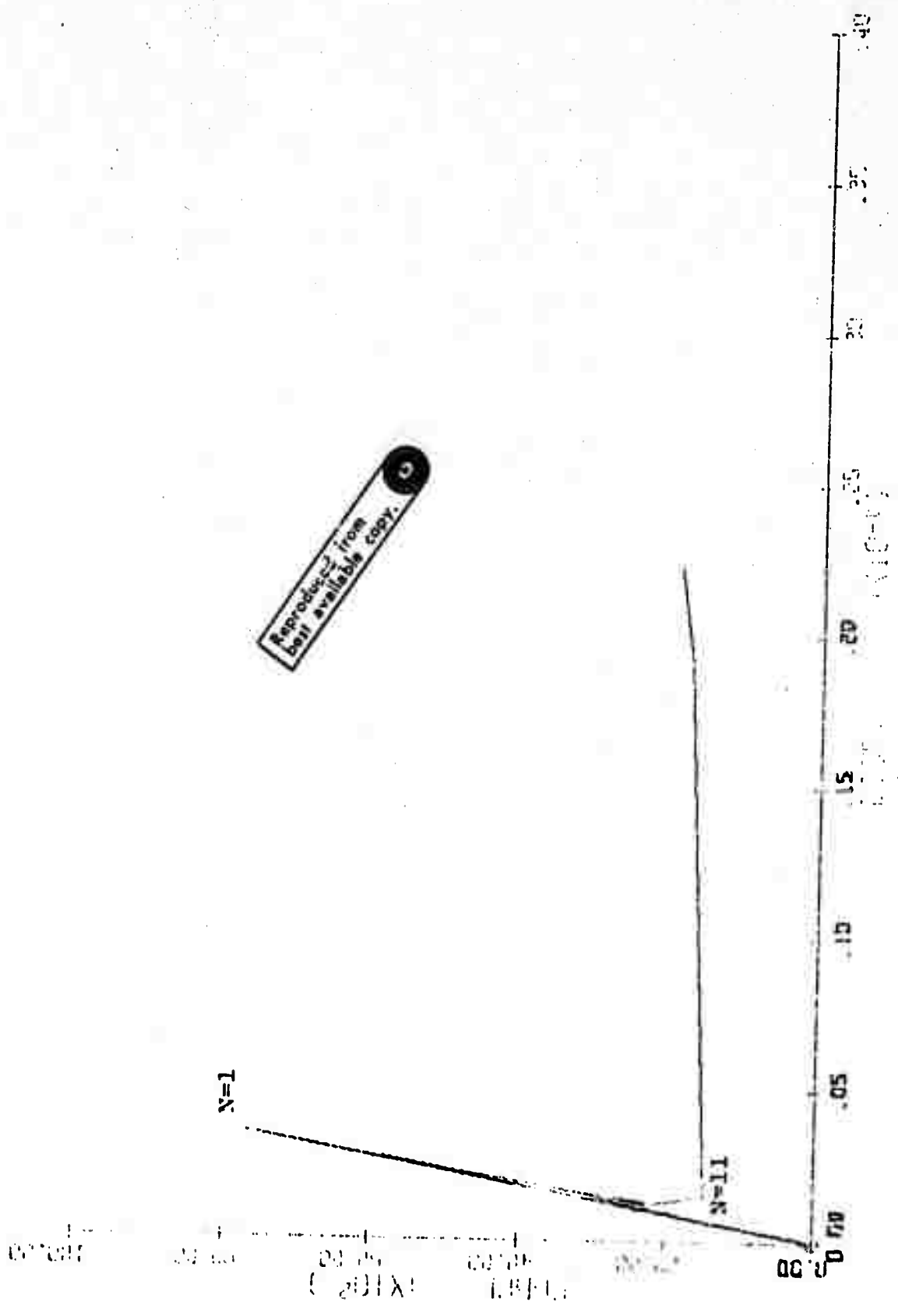


Figure 3.4.1 Progression of Failure in Test A-2



Reproduced from
best available copy.

Figure 3.4.2 Vertical Force-Displacement for Test A-2

and further results are meaningless.

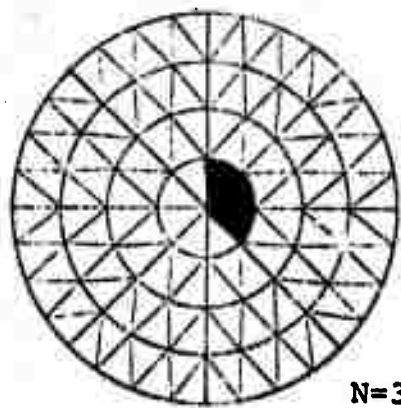
TABLE 3.4.1

BRAZILIAN TEST CONDITIONS

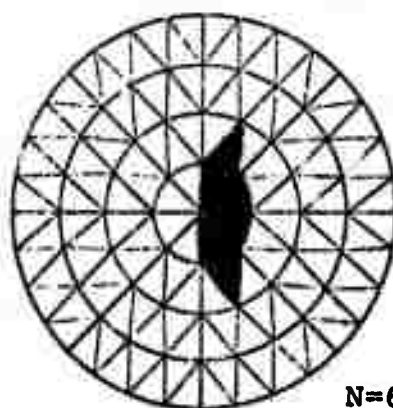
Test No.	Ratio σ_C/σ_T	No. of Loaded Nodes	Mean σ_T	Inhomogeneity
A-1	8	1	1625	Homogeneous
A-2	24	1	541.67	Homogeneous
A-3	8	3	1625	Homogeneous
A-4	24	1	541.67	Tensile strength range from 41.67 psi to 1041.67 psi
A-5	24	1	541.67	Tensile strength range from 441.67 psi to 641.67 psi
A-6	24	1	541.67	Young's modulus range from 1,600,000 psi to 13,600,000 psi

The three-point loading in test A-3 produced a tensile failure at a compressive strength-tensile strength ratio of 8. This was to be expected because a three-point loading will not create high concentration of compressive stress at the point of application of load. In Figure 3.4.3, the progressive pattern of failure is shown. Failure initiated at the center in tension and progressed simultaneously in both directions. Ultimate failure was due to wedging out of an area underneath the load which remained unfailed. The force-displacement curve is shown in Figure 3.4.4. Here, force loading would produce instant failure, but displacement loading will jump from $n = 1$ to $n = 15$ and then to ultimate failure.

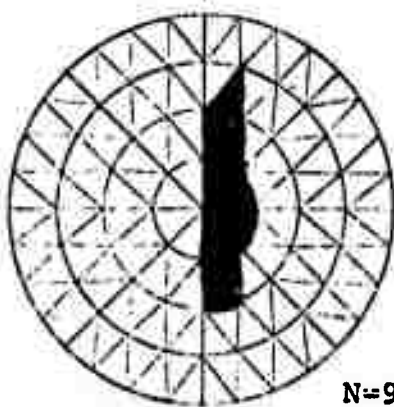
Test A-4 proved to be too inhomogeneous and failure was very scattered before ultimate failure due to crushing of the bottom load point. This rather unrealistic failure pattern, shown in Figure 3.4.5, perhaps shows that degree of inhomogeneity might be needed to be defined to model a real rock. The force-displacement behavior in Figure 3.4.6 shows another aspect of



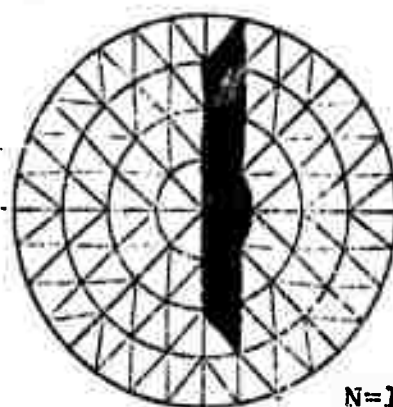
N=3



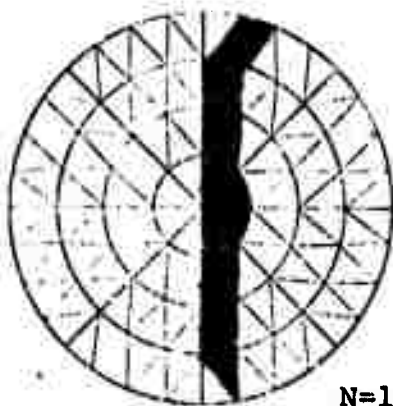
N=6



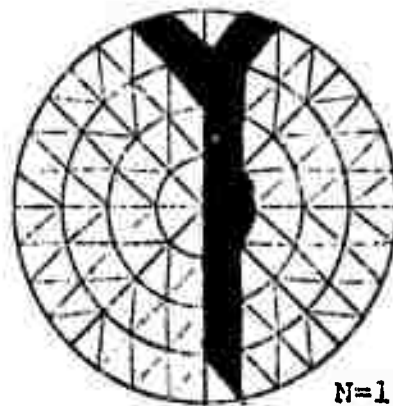
N=9



N=12



N=15



N=18

Figure 3.4.3 Progression of Failure in Test A-3

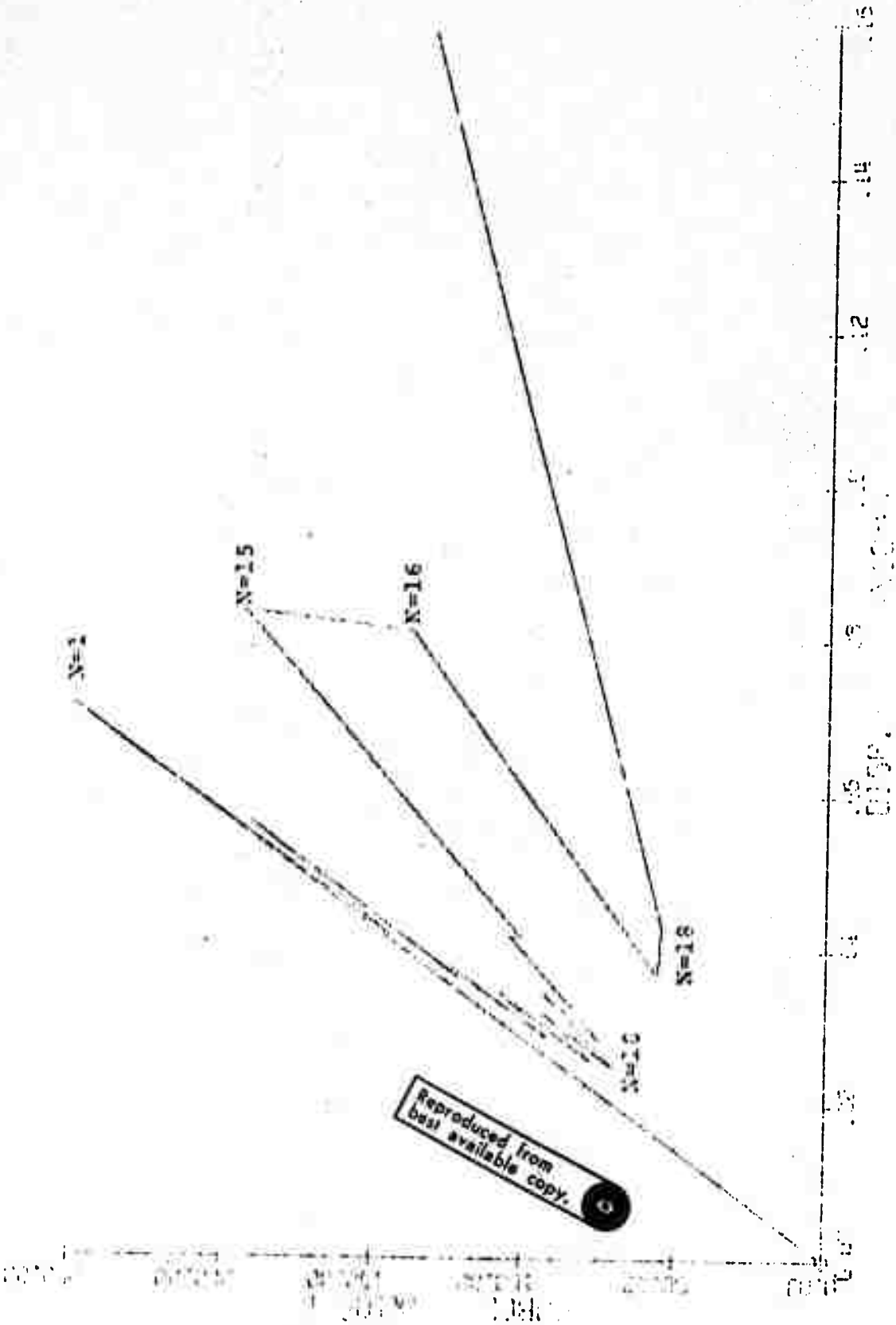


Figure 3.4.4 Vertical Force-Displacement for Test A-3

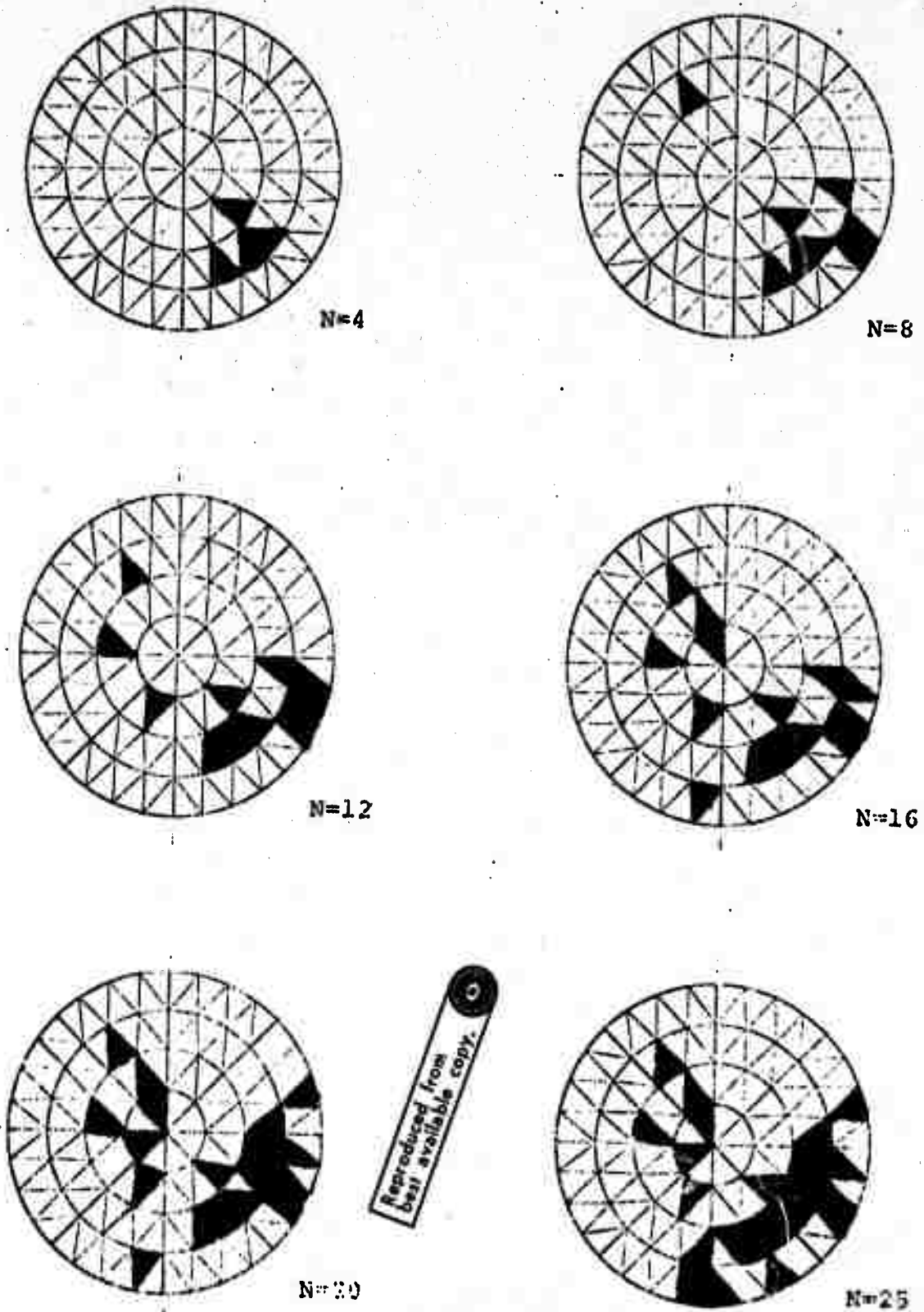


Figure 3.4.5 Progression of Failure in Test A-4

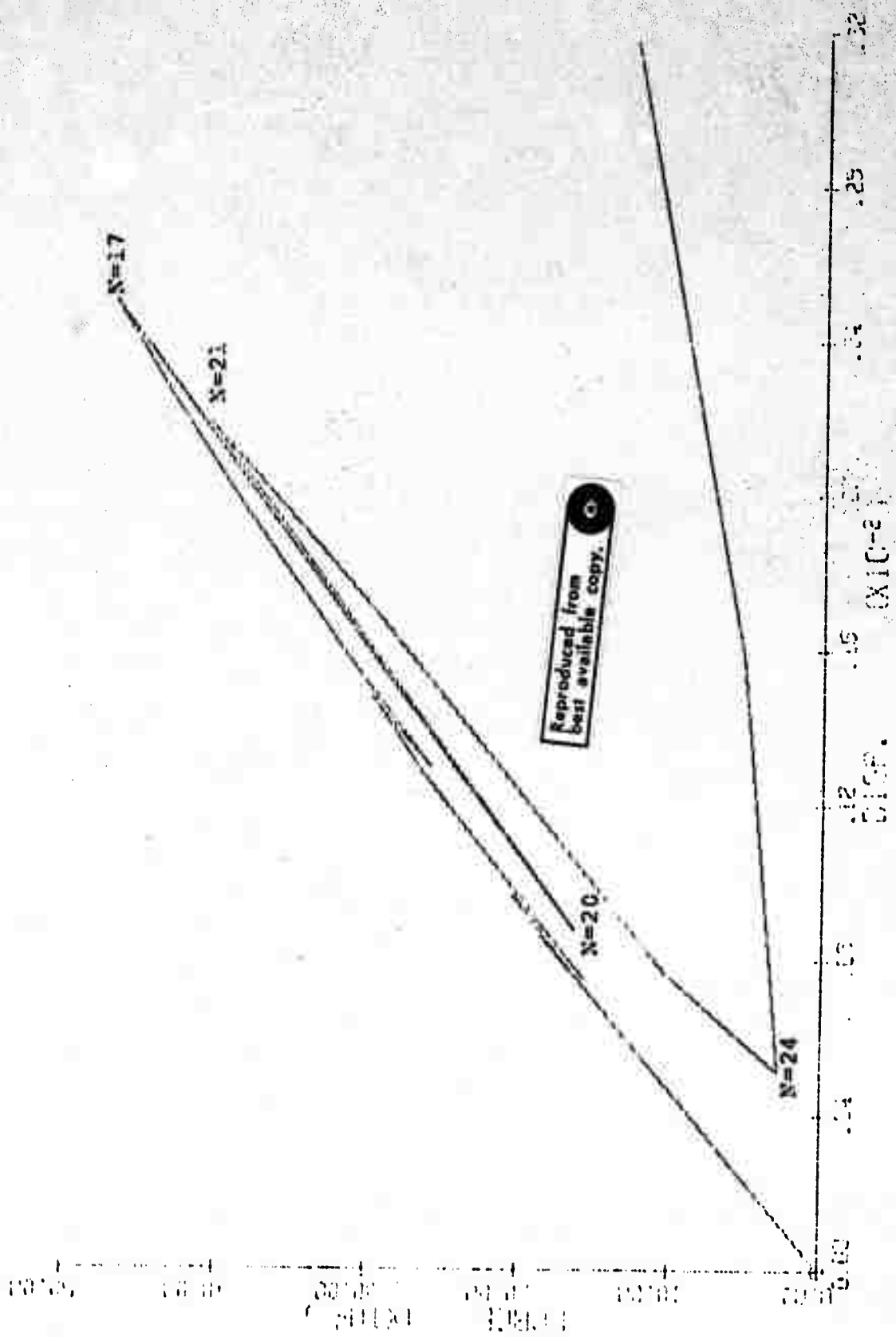


Figure 3.4.6 Vertical Force Disp for Test A-4

inhomogeneity. Failure in either force or displacement loading would not occur until 17 elements had failed.

Test A-5 was similar to test A-4 but with greatly reduced degree of inhomogeneity of the strength. In this case, the failure proceeded from the center outward but slightly to the left of the vertical diameter as shown in Figure 3.4.7. The peak force and displacement again occurred on the first element which fails indicating that failure will be instantaneous in either force or displacement loading, Figure 3.4.8.

The test of inhomogeneous modulus, test A-6, provided little new information. Even though the stiffness was highly inhomogeneous, the stress distribution appears to be similar to the homogeneous case. Apparently in the Brazilian test at least, the strength is a more sensitive variable. This was also shown to be true in case of the one-dimensional model.

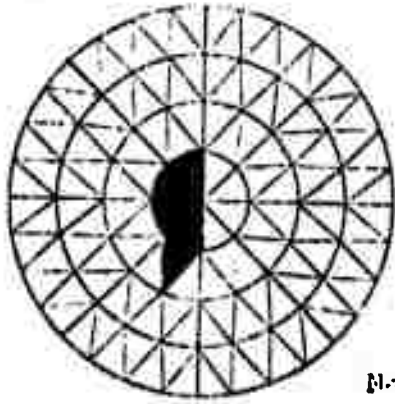
The curves of horizontal strain vs. vertical force are highly confusing as they loop back upon themselves as the specimen unloads with element failure. A typical example is shown in Figure 3.4.11.

3.5 Conclusions

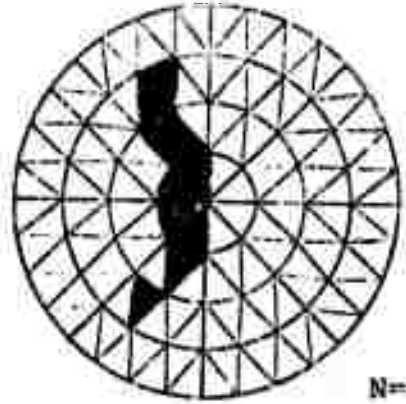
1. While the model in its present oversimplified form gives good qualitative results, it should not be considered a quantitative tool for solving rock mechanics problems until further modifications and improvisations are made.

2. Strength appears to be a more sensitive variable than stiffness. Further work is needed to determine if this is a function of the model and its assumptions or of the Brazilian test geometry.

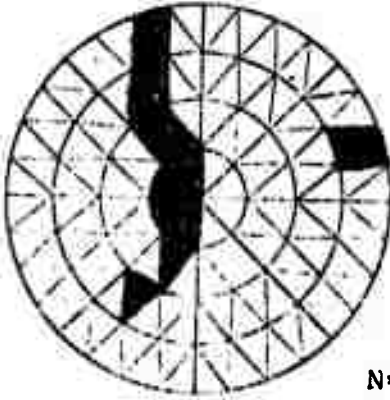
3. The model is capable of showing how failure develops in mixed stress fields. This may ultimately prove to be its most important application.



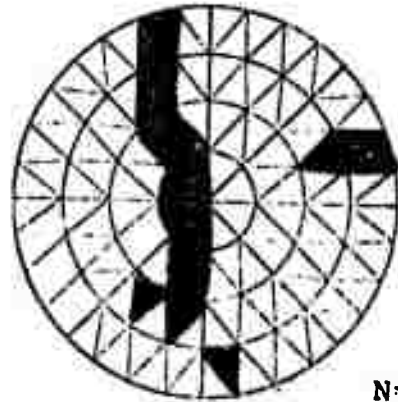
N=5



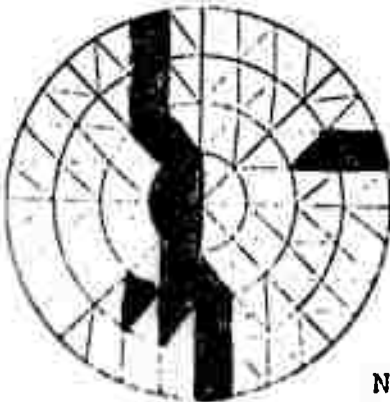
N=10



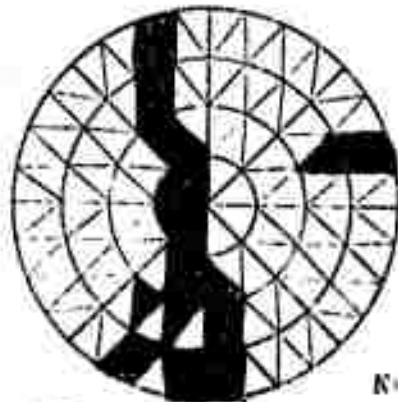
N=14



N=18



N=22



N=26

Reproduced from
best available copy.

Figure 3.4.7 Progression of Failure in Test A-5

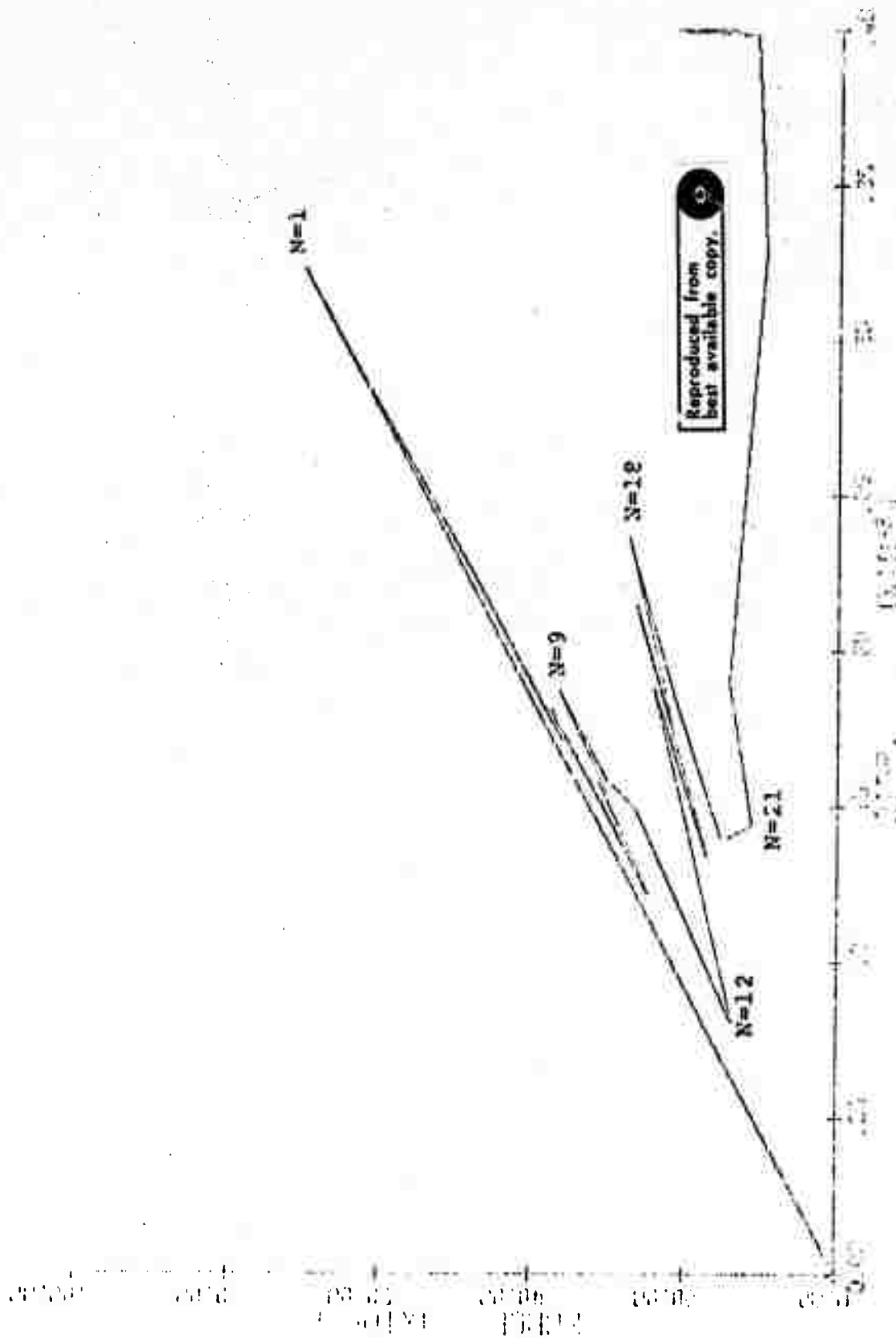


Figure 3.4.8 Vertical Force-Displacement for Test A-5

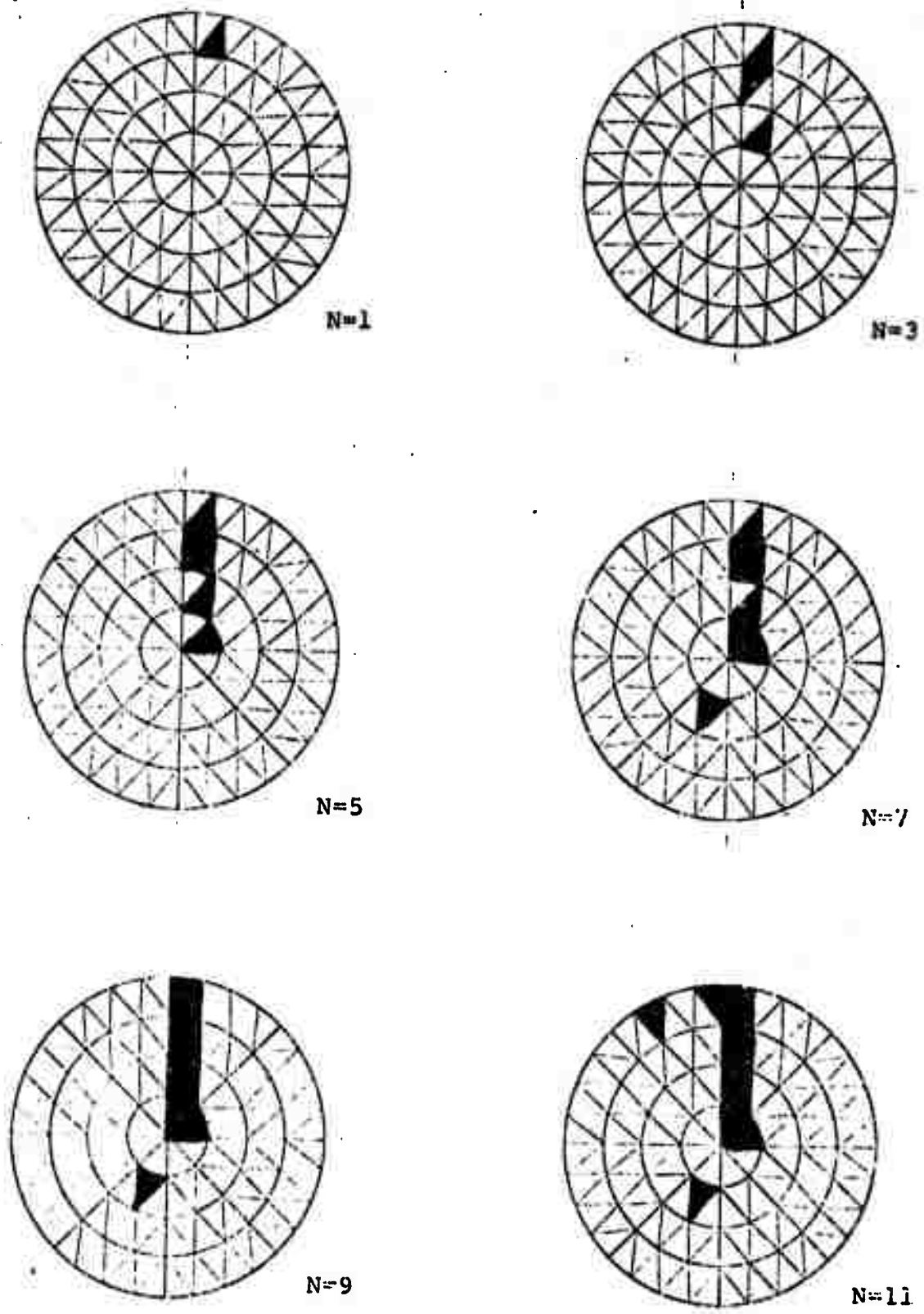


Figure 3.4.9 Progression of Failure in Test A-6

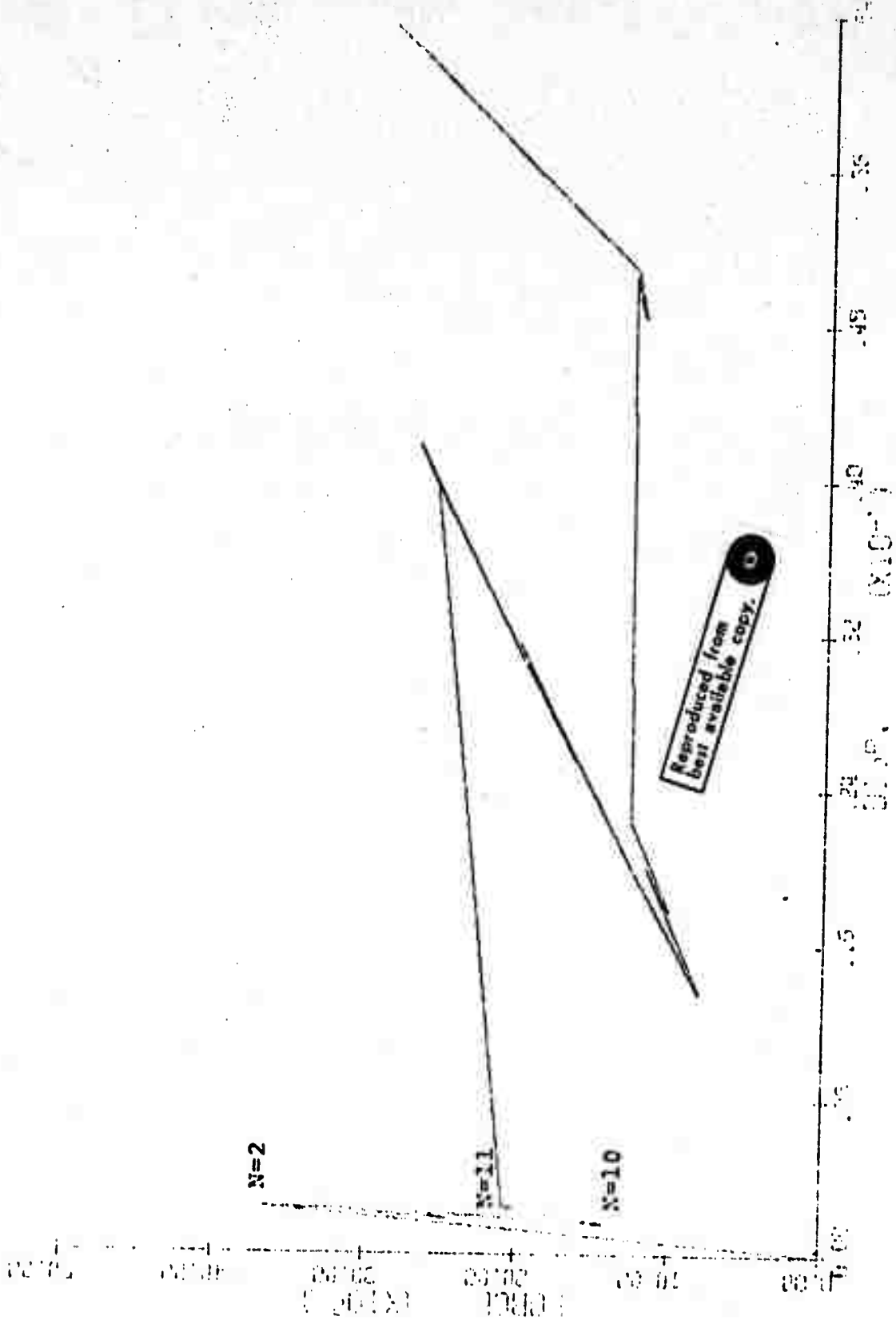


Figure 3.4.10 Vertical Force-Displacement for Test A-6

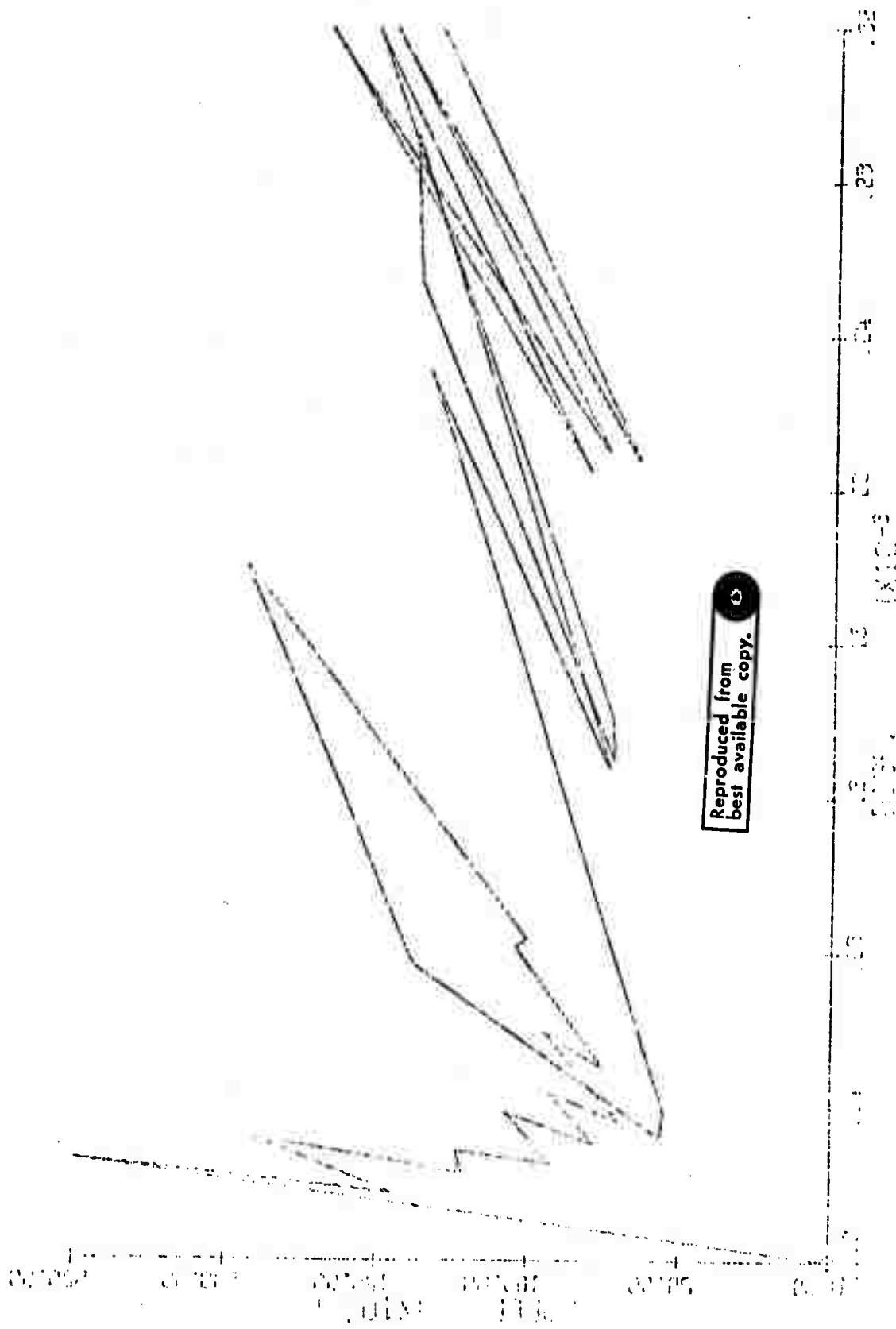


Figure 3.4.11 Vertical Force vs. Horizontal Strain for Test A-3

Bibliography

1. Su, Y. L., Y. J. Wang, and R. Stefanko, "Finite Element Analysis of Underground Stresses Utilizing Stochastically Simulated Material Properties," Eleventh Symposium on Rock Mechanics, June 1969, pp. 253-266.
2. Zienkiewicz, O. C., and Y. K. Cheung, "The Finite Element Method in Structural and Continuum Mechanics," McGraw-Hill, 1967, p. 274.
3. Hudson, J. A., E. T. Brown, and F. Rummel, "The Controlled Failure of Rock Discs and Rings Loaded in Diametral Compression," submitted to International Journal of Rock Mechanics and Mining Science.
4. Fairhurst, C., "On the Validity of the Brazilian Test for Brittle Materials," International Journal of Rock Mechanics and Mining Science, 1964, pp. 535-546.

APPENDIX A

ONE-DIMENSIONAL PROGRAM

The following pages contain a listing of the main program and seven subroutines, which were used to produce the force-displacement plots in Chapter 2. The programs contain reference to numerous subroutines provided by the Madison Academic Computing Center (MACC) as system library routines. Most of these are involved with the graphics package (2)* which produced the plots. Random numbers needed for Monte Carlo technique were obtained by MACC Library routine RANUN (3).* The operation of the program is described briefly below. While the program as presented can be run only on the Univac 1108 at MACC, it is hoped that some insights into the model can be gained from their presentation here. It is further hoped that the distribution subroutines will be useful to others interested in simulation.

The main program first fills arrays containing element stiffness (STIFF) and strength (DISM) with random variables from the appropriate distribution by calls to GENS and GENK. It computes initial total stiffness (TSTF) and uses a MACC utility routine (URSORT) to sort both arrays in ascending order of strength. In displacement loading, the force (FORCE) at each load increment is computed as the product of current total stiffness and the current displacement (DISPL). The total stiffness is then reduced by the stiffness of the failed element. The arrays (FORCE and DISPL) are then scaled and plotted.

Subroutines GENK and GENS fill arrays STIFF and DISM, respectively, with random variables by calls to appropriate distribution subroutines. These array-filling routines also compute sample statistics for comparison with distribution statistics.

The distribution subroutines (UNIFRM, UNIMOD, RSKFW, LSKEW, BIMOD) obtain random variates from the five distributions as described in

* Bibliography at the end of Chapter 2.

Chapter 2.

A list of input variables, some of which are set in the program rather than read from data cards, is given in Table A-1.

TABLE A-1

INPUT VARIABLES

- | | | | |
|----|-------|---|---|
| 1. | N | - | Total number of spring elements |
| 2. | VK | - | Stiffness variance |
| 3. | VS | - | Strength variance |
| 4. | IK | - | Code number for the stiffness distribution |
| | (1) | | Uniform distribution |
| | (2) | | Unimodal distribution |
| | (3) | | Left-skewed distribution |
| | (4) | | Right-skewed distribution, and |
| | (5) | | Bimodal distribution. |
| 5. | IS | - | Code number for the strength distribution. Same code as IK. |
| 6. | IPLOT | - | Code number for force-displacement plots |
| | (1) | | Plot not needed |
| | (2) | | Separate plots needed (e. g. , Figure 2. 4. 4) |
| | (3) | | Superimpose plots (e. g. , Figure 2. 4. 5) |
| 7. | AS | - | Minimum strength, yield point |
| 8. | NSER | - | Serial number of the data set |
| 9. | FK | - | Mean of the stiffness distribution equals $6000000./N$, for all distributions. |

```

C MAIN PROGRAM, UNFDM.....
  DIMENSION STIFF(1000),DISM(1000),DISPL(1000),FORCE(1000),
  IXDATA(10),YDATA(10),X(2),Y(2)
  EQUIVALENCE(DISM(1),DISPL(2))
  CALL INITPL(10,10,8)
  Y(1)=0.
  X(2)=30.
  Y(1)=0.
  Y(2)=100.
  1 READ 101 N,VK,VS,TK,IS,IPLUT,AS,NSFR
  IF(N.LE.0.) GO TO 10C
  PRINT 102
C FORM STIFFNESS MATRIX .....
  CALL GENK (N,TK,VK,STIFF)
C FORM STRENGTH MATRIX .....
  CALL GENK (N,IS,VS,DISM,AS)
C COMPUTE TOTAL STIFFNESS .....
  TSTF=0.
  DO 2 I=1,N
  2 TSTF=TSTF+STIFF(I)
C SORT IN ASCENDING ORDER OF STRENGTHS .....
  CALL UPSORT (1,N,DISM,STIFF,DUM1,0,DUM7)
C DISPLACEMENT LOADING .....
  PRINT 103 NSFR
  DISPL(1)=0.
  FORCE(1)=0.
  DO 3 I=2,N
  FORCE(I)=TSTF*DISPL(I)
  TSTF=TSTF-STIFF(I-1)
  3 CONTINUE
  CALL UPSRCH (0,N,FORCE,L,PEAK,0,DIJ)
  PRINT 104 L,FORCE(L),DISPL(L),DISPL(N),FORCE(2),DISPL(2)
  DO 6 I=1,N
  DISPL(I)=DISPL(I)*1000.
  C FORCE(I)=FORCE(I)*0.001
  GO TO (1,4,5),IPLUT
  4 CALL QPLUT (N1,NBLCK,P2,D3,N4)
  CALL PAGE (11,8,5,0,4HRIDFR)
  CALL SCALE (X,2,XDATA,1,6,5)
  CALL SCALE (Y,2,YDATA,1,10,5)
  CALL BASIS (2,2,XDATA,9,0,YDATA,5,90.)
  CALL PLUT (2,2,2HUP)
  XMAJ=2.
  DO 10 I=1,6
  DO 15 J=1,4
  XMIN=XMAJ+(J*0.27)
  CALL PLUT(XMIN,2,0,4HDOWN)
  CALL PLVCTR(0,0,1,4HDOWN)
  15 CALL PLUT (XMIN,2,2HUP)
  XMAJ=XMAJ+1.7
  CALL PLUT (XMAJ,2,0,4HDOWN)
  CALL PLVCTR(0,0,15,4HDOWN)
  INUM=5+I
  XNUM=XMAJ-0.1
  CALL PLNUMR(XNUM,1,7,INUM,2HT(2,0,14,0.))
  10 CALL PLUT (XMAJ,2,2HUP)
  CALL PLUT(2,2,2HUP)
  YMAJ=2.0
  DO 20 I=1,5
  DO 25 J=1,9

```

Reproduced from
best available copy.

```

YM[N]=YMAJ+(J*0.1)
CALL PLOT (2.,YMTN,4HDDWN)
CALL PLVCTR (0.1,0.,4HDDWN)
25 CALL PLOT (2.,YMTN,2HUP)
YMAJ=YMAJ+1.
CALL PLOT (2.,YMAJ,4HDDWN)
CALL PLVCTR (0.1,0.,4HDDWN)
INUM=20*I
YNUM=YMAJ-0.07
CALL PLNUMB (1.6,YNUM,INUM,2HT3,0.14,0.)
20 CALL PLOT (2.0,YMAJ,2HUP)
CALL PLTEXT (1.3,3.,*FORCE (1000 LB)55*.0.21,90.)
CALL PLTEXT (3.75,1.4,*DISPLACEMENT (.001 IN.)55*.0.21,0.)
CALL LINE (DISPL,XDATA,FORCE,YDATA,N,4HNDWF,5HSULID,6HCLUSE0)
CALL PLTEXT(2.40,6.85,*STIFFNESS DISTRIBUTION N.55*.07,0.)
CALL PLNUMB (4.25,6.85,IK,2HT1,0.07,0.)
CALL PLTEXT(2.4,6.6,*STRENGTH DISTRIBUTION N.55*.07,0.)
CALL PLNUMB(4.2,6.80,JS,2HT1,0.07,0.)
CALL PLNUMB (3.25,6.85,NSEP,2HT4,0.14,0.)
CALL PLOT (N1,NRLOK?,D2,03,N4)
PRINT 105 NRLOK,NRLOK2
GO TO 1
5 CALL LINE (DISPL,XDATA,FORCE,YDATA,N,4HNDWF,5HSULID,6HCLUSE0)
GO TO 1
C FORMAT STATEMENTS .....
101 FORMAT (I4,2F6.1,2I1,07.2,I4)
102 FORMAT (I4I)
103 FORMAT (I40,7RHDISPLACEMENT LOADING RESULTS,35X,I4)
104 FORMAT (I40,I4,10X,11HPEAK FORCE=:F7.0,10HPEAK DISP=:F9.4,
10HMAY DISP=:F9.4//14,12HYIELD FORCE=:F7.0,11HYIELD DISP=:F9.4)
105 FORMAT (I40,13HBLOCK ADDRESS,3X,T16,7X,2HT0,I16)
100 CALL ENDPLT
END

```

Reproduced from
best available copy.

```

PPINT 100,FK,VK
PRINT 100,XSAP,VARX
101 FORMAT(1H,1F(6H*****)/23H STIFFNESS DISTRIBUTION)
102 FORMAT(1H,24X,7HUNIFORM)
103 FORMAT(1H,24X,8HUNIMODAL)
104 FORMAT(1H,24X,12HRIGHT SKEWED)
105 FORMAT(1H,24X,11HLEFT SKEWED)
106 FORMAT(1H,24X,7HBI-MODAL)
107 FORMAT(24HODISTRIBUTION RANGE FROM,1PF16.8,3H TO,1PF16.8,
140X,1PF16.8)
108 FORMAT(1PHODISTRIBUTION MEAN,1PF16.8,5X,8HVARIANCE,1PF16.8)
109 FORMAT (1PHO THIS SAMPLE MEAN,1PF16.8,5X,8HVARIANCE,1PF16.8)
RETURN
END

```

Reproduced from
best available copy.

```

SUBROUTINE GENK (N,IK,VK,STIFF)
DIMENSION STIFF(N)
CALL RANUNG(NG)
FK=6000000./N
SUMX=0.
SUMX2=0.
GO TO (1,3,5,7,9),IK
1 R=EK+SQRT(7.*VK)
A=2.*EK-R
DO 2 I=1,N
CALL UNIFORM (A,R,X)
SUMX=SUMX+X
SUMX2=SUMX2+(X*X)
2 STIFF(I)=X
GO TO 11
3 R=EK+SQRT(16.*VK)
A=2.*FK-R
DO 4 I=1,N
CALL UNIFORM(A,R,X)
SUMX=SUMX+X
SUMX2=SUMX2+(X*X)
4 STIFF(I)=X
GO TO 11
5 R=EK+SQRT(2.*VK)
A=3.*FK-2.*R
DO 6 I=1,N
CALL RSKFW (A,R,X)
SUMX=SUMX+X
SUMX2=SUMX2+(X*X)
6 STIFF(I)=X
GO TO 11
7 R=EK+SQRT(8.*VK)
A=3.*EK/2.-R/2.
DO 8 I=1,N
CALL LSKFW (A,R,X)
SUMX=SUMX+X
SUMX2=SUMX2+(X*X)
8 STIFF(I)=X
GO TO 11
9 R=EK+SQRT(2.*VK)
A=2.*EK-R
DO 10 I=1,N
CALL BIMOD (A,R,X)
SUMX=SUMX+X
SUMX2=SUMX2+(X*X)
10 STIFF(I)=X
11 PRINT 101
XPAP=SUMX/N
VARX=(SUMX2/N)-(X*PAP*XPAP)
GO TO (12,13,14,15,16),IK
12 PRINT 102
GO TO 17
13 PRINT 103
GO TO 17
14 PRINT 104
GO TO 17
15 PRINT 105
GO TO 17
16 PRINT 106
17 PRINT 107,A,P,NG

```

Reproduced from
best available copy.

```

SUBROUTINE GFNS (N,IS,VS,STRNTH,A)
  DIMENSION STRNTH(N)
  SUMX=0.
  SUMX2=0.
  GO TO (1,3,5,7,9), IS
1  R=A+SQRT(17.*VS)
  ES=(A+R)/2.
  DO 2 I=1,N
  CALL UNIFORM(A,R,X)
  SUMX=SUMX+X
  SUMX2=SUMX2+(X*X)
2  STRNTH(I)=X
  GO TO 11
3  R=A+SQRT(24.*VS)
  ES=(A+R)/2.
  DO 4 I=1,N
  CALL UNIMOD(A,R,X)
  SUMX=SUMX+X
  SUMX2=SUMX2+(X*X)
4  STRNTH(I)=X
  GO TO 11
5  R=A+SQRT(18.*VS)
  ES=(2.*R+A)/3.
  DO 6 I=1,N
  CALL YSKFW (A,B,X)
  SUMX=SUMX+X
  SUMX2=SUMX2+(X*X)
6  STRNTH(I)=X
  GO TO 11
7  R=A+SQRT(18.*VS)
  ES=(2.*A+R)/3.
  DO 8 I=1,N
  CALL LSKFW (A,B,X)
  SUMX=SUMX+X
  SUMX2=SUMX2+(X*X)
8  STRNTH(I)=X
  GO TO 11
9  R=A+SQRT( 8.*VS)
  ES=(A+R)/2.
  DO 10 I=1,N
  CALL RIMOD (A,B,X)
  SUMX=SUMX+X
  SUMX2=SUMX2+(X*X)
10 STRNTH(I)=X
11 XPAR=SUMX/N
  VARX=(SUMX2/N)-(XPAR*XPAR)
  PRINT 101
  GO TO (12,13,14,15,16), IS
12 PRINT 102
  GO TO 17
13 PRINT 103
  GO TO 17
14 PRINT 104
  GO TO 17
15 PRINT 105
  GO TO 17
16 PRINT 106
17 PRINT 107,A,R
  PRINT 108,ES,VS
  PRINT 109,XPAR,VARX

```

Reproduced from
best available copy.

101 FORMAT(2PHOSTRENGTH DISTRIBUTION)
102 FORMAT(1H+.24X.7HUNIFORM)
103 FORMAT(1H+.24X.8HUNIMODAL)
104 FORMAT(1H+.24X.12HRIGHT SKEWED)
105 FORMAT(1H+.24X.11HLEFT SKEWED)
106 FORMAT(1H+.24X.7HTRIMODAL)
107 FORMAT(24HODISTRIBUTION RANGE FROM.1PF16.8.7H TO.1PE16.8)
108 FORMAT(124HODISTRIBUTION MEAN.1PF16.8.5X.8HVARIANCE.1PF16.8)
109 FORMAT(124HODISTRIBUTION THIS SAMPLE MEAN.1PF16.8.5X.8HVARIANCE.1PF16.8)
RETURN
END

Reproduced from
best available copy.



```

SUBROUTINE UNIFORM(A,B)
  R=RANUN(2)
  Y=A+(B-A)*R
  RETURN
END

```

```

SUBROUTINE UNIMOD(A,B,X)
  R1=RANUN(2)
  R2=RANUN(2)
  X=C.5*(A+B+(B-A)*(R1+R2-1.))
  RETURN
END

```

```

SUBROUTINE RSKEW(A,B,X)
  R1=RANUN(2)
  R2=RANUN(2)
  IF(R1.GE.R2) GO TO 1
  R=(2.*R2)-1.
  GO TO 2
1 R=(2.*R1)-1.
2 X=C.5*(A+B+(B-A)*R)
  RETURN
END

```

Reproduced from
best available copy.

```

SUBROUTINE LSKEW(A,B,X)
  R1=RANUN(2)
  R2=RANUN(2)
  IF(R1.GE.R2) GO TO 1
  R=(2.*R1)-1.
  GO TO 2
1 R=(2.*R2)-1.
2 X=C.5*(A+B+(B-A)*R)
  RETURN
END

```

```

SUBROUTINE BIMOD(A,B,X)
  R1=RANUN(2)
  R2=RANUN(2)
  R=R1+R2-1.
  IF(R.GE.0.) GO TO 1
  R=(1.+R)
  GO TO 2
1 R=1.-R
2 X=C.5*(A+B+(B-A)*R)
  RETURN
END

```

APPENDIX B

TWO-DIMENSIONAL PROGRAM

The following pages contain a listing of the computer program for the two-dimensional model including four required subroutines, the data deck for the Brazilian test mesh, Figure 3. 3. 1, and the plotting program with its required subroutine.

The plotting routine is self-explanatory with the documentation included in the subroutine. The subroutine EZPLOT was written for the IBM 360/44 with Calcomp Plotter and probably is not transferable to another machine. It is included for completeness only.

A list of input variables (some of which are set in the program rather than read from data cards) is given in Table B-1.

The program takes about 26 minutes of computing time on an IBM 360/44 to run completely through.

TABLE B-1

INPUT VARIABLES

1.	ISER	-	Serial number for each
2.	NPØIN	-	Number of nodes
3.	NELEM	-	Number of elements
4.	NP	-	Code number. 0 if plane strain. Anything else if plane stress.
5.	NIT	-	Number of nodes to which an external load is applied.
6.	THICK	-	Thickness
7.	RAT	-	Ratio of compressive to tensile strength
8.	X(I, 1)	-	X coordinate of I th node
	X(I, 2)	-	Y coordinate of I th node

9. U(I) - Initial load in X direction on Ith node
 V(I) - Initial load in Y direction on Ith node
 (Note that load can be force or displacement depending on value of CØDE)
10. CØDE(I) - 0 if U and V are forces, 1 if V is a force, 2 if U is a force, and 3 if U and V are displacements. If code is greater than three, that node is a loaded node and four is subtracted from its code before the code is used by the program.
11. EP(I, 1) - Modulus of elasticity
 EP(I, 2) - Poisson's ratio
 EP(I, 3) - Tensile strength for Ith element
12. A and B - Minimum and maximum value, respectively, for modulus of elasticity, defined in the subroutine CARDS
13. C and D - Minimum and maximum value, respectively, for tensile strength, defined in the subroutine CARDS

```

C** FINITE ELEMENT ANALYSIS PROGRAM
C** COMMON C(6,6),DBA(128,3,6),B(3,6)/GEV/EP(128,3)
C** DIMENSION X(81,2),XE(3,2),NDD(128,3),U(81),V(81),CODE(51),
C** 1ST(162,36),KK(6),P(162),DIS(6),STR(3),PRI(3),F(5),
C** 21NODE(5)
C** READ AND PRINT DATA
C** READ (5,90C) NPOIN,NELEM,NP,NIT,THICK,RAI,ISER
C** WRITE (6,90C) NPOIN,NELEM,NP,NIT,THICK,RAI,ISER
C** J=1
C** M BAND=30
C** DO 30 I=1,NPOIN
C** READ (5,920) X(I,1),X(I,2),U(I),V(I),CODE(I)
C** WRITE (6,92C) X(I,1),X(I,2),U(I),V(I),CODE(I)
C** IF (CODE(I).LE.3.) GO TO 30
C** ITNODE(J)=I
C** J=J+1
C** JCODE(I)=CODE(I)-4.
C** CONTINUE (6,970)
C** READ (5,91C) NCARD
C** IF (NCARD.EC.NPOIN) GO TO 35
C** WRITE (6,94C)
C** GO TO 1000
C** DO 40 I=1,NELEM
C** READ (5,910) (NOD(I,J),J=1,3)
C** WRITE (6,910) (NOD(I,J),J=1,3)
C** READ (5,91C) NCARD
C** IF (NCARD.EC.NELEM) GO TO 100
C** WRITE (6,950)
C** GO TO 1000
C** INITIALIZE STIFFNESS AND B MATRICES
C** DO 100 DO 320 J=1,6
C** DO 320 I=1,6
C** B(1,J)=0.
C** B(3,3)=1.
C** B(3,5)=1.
C** CALL OI (I,J)
C** DO 101 I=1,NELEM
C** OI=I(6,980)EP(LL,1),EP(LL,2),EP(LL,3)

```

Reproduced from
 best available copy.



```

101 CONTINUE
300 NPOIN2=NPOIN#2
   DO 310 I=1,NPOIN2
   DO 310 J=1,M6AND
31C ST(I,J)=0.
C ***** STIFFNESS MATRIX *****
C FORM STIFFNESS MATRIX *****
C ***** LK=1,NELEM *****
   DO 430 I=1,3
   JJ=NOD(LK,I)
   XE(I,1)=X(JJ,1)
410 YM=EP(LK,1)
   PR=EP(LK,2)
   CALL FEM(XE,YM,PR,THICK,NP,LK)
   KK(1)=2*NOD(LK,1)
   KK(2)=2*NOD(LK,2)
   KK(3)=2*NOD(LK,3)
   KK(4)=2*NOD(LK,4)
   KK(5)=2*NOD(LK,5)
   KK(6)=2*NOD(LK,6)
   DO 420 I=1,6
   II=KK(I)
   DO 420 J=1,6
   IF(KK(J).LI.II) GO TO 420
   JJ=KK(J)-II+1
   ST(I,JJ)=ST(II,JJ)+C(I,J)
420 CONTINUE
430 CONTINUE
   WRITE (6,970)
   WRITE (8) ((ST(I,J),I=1,NPOIN2),J=1,M6AND)
   REWIND 8
C ***** BOUNDARY CONDITIONS AND MODIFY STIFFNESS MATRIX *****
C IMPOSE *****
C ***** IJ=CODE(N) *****
500 R(I)=0.
   DO 590 N=1,NPOIN
   NN=2*N-1
   IJ=CODE(N)
   JJ=1
   CO=J(N)
   R(NN)=R(NN)+CO
   R(NN+1)=R(NN+1)+V(N)
   IF(IJ.EQ.0) GO TO 590
   GO TO (550,530,510),IJ

```

```

530 NN=NN+1
    CO =V(N)
    GO TO 550
540 JJ=2
550 DO 580 I=1, JJ
      DO 570 M=2, MBAND
        K=NN-M+1
        IF (K.LE.C) GO TO 560
        R(K)=R(K)-ST(K,M)*CO
        ST(K,M)=0.
560 K=NN+M-1
      IF (K.GT.NPCIN2) GO TO 570
      R(K)=R(K)-ST(NN,M)*CO
      ST(NN,M)=0.
570 CONTINUE
      ST(NN,1)=1.
      R(NN)=CO
      CO=V(N)
580 NN=NN+1
590 CONTINUE
C***** SOLVE EQUATIONS *****
C***** DO 690 N=1, NPCIN2 *****
C***** IF (ST(N,L).EQ.0.) GO TO 670 *****
      I=N+L-1
      CO=ST(N,L)/ST(N,1)
      J=0
      DO 650 K=L, MBAND
        J=J+1
        ST(I,J)=ST(I,J)-CO*ST(N,K)
650 ST(N,L)=CO
        R(I)=R(I)-CO*R(N)
670 CONTINUE
      DO 655 M=2, NPCIN2
        N=NPONIN2+1-M
        DO 655 L=2, MBAND
          IF (ST(N,L).EQ.0.) GO TO 655
          K=N+L-1
          R(N)=R(N)-ST(N,L)*R(K)
655 CONTINUE
C***** COMPUTE STRESSES *****
C***** WORAT=0. *****
      DO 930 LL=1, NELEM

```

Reproduced from
best available copy.

```

DO 810 I=1,3
JJ=NOD(LL,I)=K(2#JJ-1)
DIS(2#I)=R(2#JJ)
DO 820 I=1,3
STR(I)=0.
DO 320 K=1,6
STR(I)=STR(I)+DBA(LL,I,K)*DIS(K)
CALL PRIN (STR,PRI)
TSTREN=EP(LL,3)
CSTRN=-RAT#TSTREN
RAT1=PRI(1)/TSTREN
RAT2=PRI(2)/CSTRN
IF(RAT1.GT.WORAT) GO TO 821
IF(RAT2.GT.WORAT) GO TO 823
GO TO 830
821 WORAT=RAT1
LFAIL=LL
GO TO 822
823 WORAT=RAT2
LFAIL=L:
830 CONTINUE
831 TFORCE =0.
845 DO 845 I=1,5
F(I)=0.
DO 840 I=1,NPCIN2
R(I)=R(I)/WORAT
DISP=R(10)
STRAIN=(R(83)-R(9))/29
V(I)=0.
U(I)=0.
DO 849 II=1,NIT
KN=ITNDE(II)
V(KN)=2
READ (8) ((ST(I,J),I=1,NPCIN2),J=1,MBAND)
REWIND 8
DO 850 I=1,NIT
J=2#ITNODF(I)
K=J+1
DO 860 L=1,J
L2=K-L
F(I)=F(I)+ST(L,L2)*R(L)
LEFT=NPICIN2-J
IF(LEFT+1.GT.MBAND) LEFT=MBAND-1
DO 870 L=1,LEFT
F(I)=F(I)+ST(J,L+1)*R(J+L)
850 TFORCE =TFORCE+F(I)

```

Reproduced from
best available copy.

```

WRITE (6,960) LFAIL,DISP ,TFORCE,STRAIN
WRITE (9,920) DISP ,TFORCE,STRAIN
DO 1110 I=1,3
JJ=NOD(LFAIL,I)
XE(I,1)=X(JJ,1)
XE(I,2)=X(JJ,2)
YM=EP(LFAIL,1)*.99
PR=EP(LFAIL,2)
CALL FEM(XE,YM,PK,THICK,NP,LFAIL)
KK(2)=2*NOD(LFAIL,1)
KK(1)=KK(2)-1
KK(4)=2*NOD(LFAIL,2)
KK(3)=KK(4)-1
KK(6)=2*NOD(LFAIL,3)
KK(5)=KK(6)-1
DO 1120 I=1,6
II=KK(I)
DO 1120 J=1,6
IF(KK(J).LT.II) GO TO 1120
JJ=KK(J)-II+1
ST(II,JJ)=ST(II,JJ)-C(I,J)
CONTINUE
DO 1115 I=1,3
DO 1115 J=1,6
DBA(LFAIL,I,J)=0.
1115 CONTINUE
C***** STATEMENTS *****
C***** (414,2F16.8,I4) *****
C***** (314) *****
C***** (3F16.8) *****
C***** (26HRONG *****
C***** (29HRONG *****
C***** (1H,30X,I4,3F16.8) *****
C***** (1H0,77) *****
C***** (3F16.2) *****
900 FORMAT
910 FORMAT
920 FORMAT
540 FORMAT
950 FORMAT
560 FORMAT
570 FORMAT
590 FORMAT
1000 STOP
END

```

Reproduced from
 best available copy.

END OF FILE REACHED ON INPUT UP END OF EXTENT ON OUTPUT

```

SUBROUTINE FEM (XF, YM, PR, THICK, NP, N)
DIMENSION XF(3,2), ZX(3), ZY(3), A(6,6), B(3,6),
CCMNCN C(6,6), DBA(128,3,6), B(3,6), D(3,3), DB(3,6), BTDBA(6,6)
DO 20 J=1,6
DO 21 I=1,3
EB(I,J) = 0.
DO 20 I=1,6
A(I,J) = 0.
BTDBA(I,J) = 0.
DO 22 J=1,3
DO 22 I=1,3
D(I,J) = 0.
ORX = (XF(1,1)+XF(2,1)+XF(3,1))/3.
DO 5 I=1,3
XE(I,1) = XE(1,1) - ORX
XE(I,2) = XE(2,1) - ORX
ZX(1) = XE(2,2) - XE(3,2)
ZX(2) = XE(3,2) - XE(1,2)
ZX(3) = XE(1,2) - XE(2,2)
ZY(1) = XE(3,1) - XE(2,1)
ZY(2) = XE(2,1) - XE(3,1)
ZY(3) = XE(1,1) - XE(2,1)
ZK = XE(2,1)*XE(3,2) - XE(3,1)*XF(2,2)
A(1,1) = 1./3.
A(2,1) = ZX(1)/Z
A(3,1) = ZY(1)/Z
A(4,2) = A(2,1)
A(5,2) = A(3,1)
A(6,2) = 1./3.
A(1,3) = ZX(2)/Z
A(3,3) = ZY(2)/Z
A(4,4) = A(2,3)
A(5,4) = A(3,3)
A(6,4) = 1./3.
A(1,5) = ZX(3)/Z
A(3,5) = ZY(3)/Z
A(4,6) = A(2,5)
A(5,6) = A(3,5)
A(6,6) = A(3,5)
IF (NP) 75, 81, 75

```

```

C C C
81 ***** ELASTICITY MATRIX FOR PLANE STRAIN CASE *****
   D(1,1) = (YM*PR)/(1-PR*PR) *****
   D(2,1) = D(1,1) *****
   D(1,2) = D(2,1) *****
   D(2,2) = D(1,2) *****
   D(3,3) = (YM*2*YM*PR)/(2*(1-PR-2.*PK*PR)) *****
GO TO 72 *****
C C C
75 ***** ELASTICITY MATRIX FOR PLANE STRESS CASE *****
   D(1,1) = YM/(1-PR*PR) *****
   D(2,1) = D(1,1) *****
   D(1,2) = D(2,1) *****
   D(2,2) = D(1,2) *****
   D(3,3) = YM/(2*(1+PR)) *****
72 DO 30 J=1,6 *****
DO 30 I=1,3 *****
DO 30 K=1,3 *****
DO 40 J=1,6 *****
DO 40 I=1,6 *****
DO 40 K=1,6 *****
40 DBA(N,I,J)=DB(I,K)*A(K,J) *****
***** STRESS MATRIX IS FORMED *****
***** VOL=.5*THICK*Z *****
DO 50 J=1,6 *****
DO 50 I=1,6 *****
DO 50 K=1,3 *****
50 BTDBA(I,J)=BTDBA(I,J)+B(K,I)*DBA(N,K,J)*VCL *****
DO 60 J=1,6 *****
DO 60 I=1,6 *****
DO 60 K=1,3 *****
60 C(I,J)=C(I,J)+A(K,I)*BTDBA(K,J) *****
***** STIFFNESS MATRIX C IS FORMED *****
***** RETURN *****
C C C
END

```

```

SUBROUTINE PRIN(D,C)
DIMENSION D(3),C(3)
C(1)=(D(1)+D(2))*5+SQRT((D(1)-D(2))**2/4.+D(3)**2)
C(2)=(D(1)+D(2))*5-SQRT((D(1)-D(2))**2/4.+D(3)**2)
RETURN
END

```

```

SUBROUTINE CARDS (N,C)
COMMON /GEN/ EP(128,3)
A=1600000.
B=13600000.
C=41.3367
D=1041.3367
DO 20 I=1,N
EP ( I,2) =0.25
CALL UNIFORM (A,B,X)
CALL UNIFORM (C,D,Z)
EP(I,3)=Z
EP(I,1)=X
RETURN
END

```

20

```

SUBROUTINE UNIFORM (A,B,X)
R = RANDOM (I)
X=A+(B-A)*R
RETURN
END

```

```

C*****
C PLOTTING PROGRAM
C
C PLOTS VERTICAL FORCE VS. VERTICAL DISPLACEMENT AND
C VERTICAL FORCE VS. HORIZONTAL STRAIN
C*****
C DIMENSION X(129),Y(129),XX(2),YY(2),Z(129)
C XX(1)=3.
C XX(2)=-.03
C YY(1)=0.
C YY(2)=10000.
C X(1)=0.
C Y(1)=0.
C Z(1)=0.
C N=9999
C XLEN=8
C YLEN=5
C CALL EZPLTL (XX,YY,N,XLEN,YLEN)
C CALL EZPLOT (XX,YY,-1)
C DO 10 I=2,82
C READ(9,100)X(I),Y(I),Z(I)
C WRITE(6,100) X(I),Y(I),Z(I)
C X(I)=-X(I)
C Y(I)=-Y(I)
C 10 CONTINUE
C CALL EZPLOT (X,Y,-1)
C XX(1)=0.
C XX(2)=-.0003
C CALL EZPLTL (XX,YY,N,XLEN,YLEN)
C CALL EZPLOT (Z,Y,-1)
C CALL PLOT (15,0,-2.1,-3)
C FORMAT(3F16.8)
C 100 END

```

```

C-----
C SUBROUTINE EZPLOT(X,Y,M)
C-----
C PROGRAM TO PLOT X-Y DATA ON CALCOMP, SEVERAL DEPENDENT-VARIABLE
C ARRAYS CAN BE PLOTTED AS A FUNCTION OF THE INDEPENDENT VARIABLE.
C
C DESCRIPTION OF PARAMETERS---
C X--INDEPENDENT-VARIABLE ARRAY.
C Y--DEPENDENT-VARIABLE ARRAY.
C M--NUMBER OF X-Y PAIRS,NEGATIVE VALUE PLOTS X-Y ON PREVIOUS PLOT.
C-----
EZPLT 1
EZPLT 3
EZPLT 4
EZPLT 5
EZPLT 6
EZPLT 7
EZPLT 8
EZPLT 9
EZPLT 10

```



```

5 IF(N.GT.0) GO TO 15
C ADDITIONAL PLOT ON PREVIOUS AXES.
N=-N
JSYMB=MOD(JSYMB+1,6)
IF(IOS.EQ.0) GO TO 25
IF(IOS.EQ.1) NS=-MAXC(1,IAES(N/41))
IOS=IOS+1
NS=C
GO TO 25
C NEW PLOT, ADVANCE PAPER AND PLOT AXES.
15 JSYMB=1
XL=XLEN
YL=YLEN
IOS=0
IF(N.NE.9999) GO TO 20
IOR=1
IOS=1
JSYMB=0
20 CALL PLOT(PX+3.0,0.0,-3)
ICN=ICN+1
DUMX(1)=X(1)
DUMX(2)=X(N)
DUMY(1)=Y(1)
DUMY(2)=Y(N)
IF(N.EQ.2) GO TO 23
DO 22 I=1,N
DUMX(1)=AMINI(DUMX(1),X(I))
DUMX(2)=AMAXI(DUMX(2),X(I))
DUMY(1)=AMINI(DUMY(1),Y(I))
DUMY(2)=AMAXI(DUMY(2),Y(I))
23 CALL SCALE(DUMX,XL,2,1,10.)
MIC=MOD(ICN,10)
IF(MIC.EQ.0) MIC=10
TXN(2)=LOG(MIC)
IF(ICN.LT.10) GO TO 9876
MID=MOD(ICN/10,10)
IF(MID.EQ.0) MID=10
TXN(1)=LOG(MID)
IF(ICN.LT.100) GO TO 9876
TXN(3)=TXN(2)
TXN(2)=TXN(1)
MIF=MOD(ICN/100,10)
IF(MIF.EQ.0) MIF=10
TXN(1)=LOG(MIF)
C CONTINUE
9876 CALL AXIS(0.0,0.0,IX, -11,XL,0.,X3,X4,10.0)

```

Reproduced from
best available copy.

60
EZPLT 61
EZPLT 62
EZPLT 63
EZPLT 64
EZPLT 65
EZPLT 66
EZPLT 67
EZPLT 68
EZPLT 69
EZPLT 70
EZPLT 71
EZPLT 72
EZPLT 73
EZPLT 74
EZPLT 75
EZPLT 76
EZPLT 77
EZPLT 78
EZPLT 79
EZPLT 80
EZPLT 81
EZPLT 82
EZPLT 83
EZPLT 84
EZPLT 85
EZPLT 86
EZPLT 87
EZPLT 88
EZPLT 89
EZPLT 90
EZPLT 91
EZPLT 92
EZPLT 93
EZPLT 94
EZPLT 95
EZPLT 96
EZPLT 97
EZPLT 98
EZPLT 99
EZPLT 100
EZPLT 101
EZPLT 102
EZPLT 103
EZPLT 104
EZPLT 105
EZPLT 106
EZPLT 107

```

CALL SCALE(DUMY, YL, 2, 1, 10.)
CALL AXIS(0., 0., TY, 8, YL, 90., Y3, Y4, 10., 0)
IF(IOR.EQ.1) RETURN
CALL WHERE(XP, YP, DUM)
ISW=0
25  C FIND WHICH END OF ARRAY IS CLOSER TO PEN POSITION.
    $ IF((XP-XD(X(1)))**2+(YP-YD(Y(1)))**2.GT.
      (XP-XD(X(N)))**2+(YP-YD(Y(N)))**2) ISW=1
      J=1+ISW*(N-1)
      XX=AMAX1(0., (AMINI(XL, XD(X(J))))))
      YY=AMAX1(0., (AMINI(YL, YD(Y(J))))))
      CALL PLOT(XX, YY, 3)
      DD 30 I=1, N
      J=ISW*(N+1-2*I)+1
C
PLOT WILD POINTS AT BORDERS
XX=AMAX1(0., (AMINI(XL, XD(X(J))))))
YY=AMAX1(0., (AMINI(YL, YD(Y(J))))))
IF(NS.GE.0) CALL PLOT(XX, YY, 2)
IF(NS.EQ.0) GO TO 30
CALL SYMBOL(XX, YY, 0.08, JSYMB, 0.0, -1)
30  CONTINUE
    RETURN
    END
EZPLT1108
EZPLT1109
EZPLT1110
EZPLT1111
EZPLT1112
EZPLT1113
EZPLT1114
EZPLT1115
EZPLT1116
EZPLT1117
EZPLT1118
EZPLT1119
EZPLT1120
EZPLT1121
EZPLT1122
EZPLT1123
EZPLT1124
EZPLT1125
EZPLT1126
EZPLT1127
EZPLT1128
EZPLT1129
EZPLT1130
EZPLT1131
EZPLT1132

```


62 721 710 70 69 68 68 67 66 56 47 47 38 29 19 10 11 12 5 6 6 7 7 8 8 9 26 27 27 6 6 5 4 5 4 3 3 7 3 7 4

72 71 70 59 68 58 67 66 56 47 49 38 29 30 19 20 11 12 23 1 6 1 5 8 1 9 2 2 5 7 2 5 6 4 5 4 5 3 3 2 2 3 2 7 4 1

61 60 60 59 59 58 57 57 48 48 39 39 30 20 20 21 22 1 1 3 4 1 5 1 6 1 6 2 5 5 5 4 4 4 4 3 3 2 3 7 2

81 80 79 78 77 76 75 65 64 64 55 46 47 38 28 18 17 12 23 34 4

71 70 69 77 68 67 65 64 55 46 37 28 18 17 10 1 2 13 12 13 5

72 71 70 69 69 68 67 66 66 56 47 38 38 29 19 10 10 11 12 13 128